Agonist-promoted ubiquitination differentially regulates receptor trafficking of endothelin type A and type B receptors

Koji Terada[1], Takahiro Horinouchi[1], Yoichiro Fujioka[2], Tsunehito Higashi[1], Prabha Nepal[1], Mika Horiguchi[1], Sarita Karki[1], Chizuru Hatate[1], Akimasa Hoshi[1], Takuya Harada[1], Yosuke Mai[1], Yusuke Ohba[2] and Soichi Miwa[1]

[1]Department of Cellular Pharmacology, Hokkaido University Graduate School of Medicine, North 15, West 7, Kita-ku, Sapporo 060-8638, Japan. [2]Department of Cell Physiology, Hokkaido University Graduate School of Medicine, North 15, West 7, Kita-ku, Sapporo 060-8638, Japan.

*Running title: *Endothelin type A and B receptor ubiquitination and trafficking*

To whom correspondence should be addressed: Soichi Miwa, Department of Cellular Pharmacology, Hokkaido University Graduate School of Medicine, North 15, West 7, Kita-ku, Sapporo 060-8638, Japan.
Tel: +81-11-706-6921; Fax: +81-11-706-7824
E-mail: smiwa@med.hokudai.ac.jp

Keywords: G protein coupled receptor; endothelin receptor; ubiquitination; internalization; trafficking

Background: Agonist-stimulation induces different intracellular trafficking of endothelin receptors ($ET_{A/B}R$) after internalization. The mechanism is unclear.
Results: Stimulation induces ubiquitination, lysosomal targeting and decreased cell surface ET_BR levels. Non-ubiquitinated ET_AR and ET_BR mutant recycled to plasma membrane with smaller changes in the levels.
Conclusion: Ubiquitination determines intracellular trafficking of endothelin receptors.
Significance: ET_BR ubiquitination fine-tunes cellular responses to agonist, by regulating cellular receptor levels.

ABSTRACT

Two types of G protein-coupled receptors for endothelin-1 (ET-1), ET type A receptor (ET_AR) and ET_BR, closely resemble each other, but upon ET-1 stimulation, they follow totally different intracellular trafficking pathways: ET_AR is recycled back to plasma membrane, whereas ET_BR is targeted to lysosome for degradation. However, mechanisms for such different fates are unknown. Here we demonstrated that ET_BR but not ET_AR was ubiquitinated on cell surface following ET-1 stimulation, and that ET_BR was internalized and degraded in lysosome more rapidly than ET_AR. The mutant ET_BR (designated "5KR mutant") in which 5 lysine residues in C-tail were substituted to arginine was not ubiquitinated, and its rates of internalization and degradation after ET-1 stimulation became slower, being comparable to that of ET_AR. Confocal microscopic study showed that following ET-1 stimulation, ET_AR and 5KR mutant of ET_BR were co-localized mainly with Rab11, a marker of recycling endosome, whereas ET_BR was with Rab7, a marker of late endosome/lysosome. In 5KR mutant, ET-1-induced ERK phosphorylation and an

increase in the intracellular Ca^{2+} concentration upon repetitive ET-1 stimulation were larger. A series of ET_BR mutants (designated "4KR mutant") in which either one of 5 arginine residues of the 5KR mutant was reverted to lysine were normally ubiquitinated, internalized and degraded, with ERK phosphorylation being normalized. These results demonstrate that agonist-induced ubiquitination at either lysine residue in C-tail of ET_BR but not ET_AR switches intracellular trafficking from recycling to plasma membrane to targeting to lysosome, causing decreases in cell surface level of ET_BR and intracellular signaling.

Endothelin-1 (ET-1) is a vasoconstricting peptide of 21 amino acids, which is synthesized and released in endothelial cells (1). ET-1 is considered to play an important role in the physiological control of blood pressure and cardiac function and also in genesis and development of cardiovascular diseases such as atherosclerosis (2), cardiac remodeling accompanying chronic heart failure (3), and pulmonary arterial hypertension (4). There are two types of receptors for ET-1: endothelin type A receptor (ET_AR) and ET_BR, both of which are G protein-coupled receptors (GPCRs) (5,6). ET_AR is coupled with Gq and Gs (7,8), while ET_BR is coupled with Gq and Gi (7,9). Typically, ET_AR is present on vascular smooth muscle cells and upon agonist stimulation, it induces contraction of the cells to cause vasoconstriction. On the other hand, ET_BR is present on vascular endothelial cells and upon agonist stimulation, it induces nitric oxide production through activation of endothelial nitric oxide synthase to cause vascular relaxation (10). ET_BR is also known to function as a clearance receptor for ET-1, which removes ET-1 from the extracellular fluid by binding ET-1 and rapidly internalizing into the inside of the cell (11,12).

Administration of a receptor agonist ET-1 to whole animals is reported to induce a transient decrease in the blood pressure resulting from vasodilatation via ET_BR, followed by a long-lasting increase in the blood pressure resulting from vasoconstriction via ET_AR. The biphasic change in the blood pressure is considered to result from rapid desensitization of ET_BR-mediated response and negligible desensitization of ET_AR-mediated response (1,12,13).

The different susceptibility to desensitization of ET_AR- and ET_BR-mediated responses could be explained mainly by different intracellular trafficking of both receptors after stimulation with their agonist ET-1 (14,15), although ET_AR and ET_BR closely resemble each other (≈55% overall; 77% within the putative transmembrane helices) (16,17). Upon agonist stimulation, both receptor subtypes are rapidly internalized to early endosome, but subsequently targeted to different intracellular destinations (14,18). ET_AR is recycled back to the plasma membrane through the pericentriolar recycling compartment, while ET_BR is targeted to lysosomes for degradation through late endosome (14,18).

Several lines of evidence indicate that cytoplasmic carboxyl terminal tail (C-tail) determines the pathway of agonist-induced trafficking of several GPCRs including endothelin receptors (ETRs) (19,20). With respect to ETRs, this conclusion is based on the studies using chimeric mutants of ETRs where the C-tails of ET_AR and ET_BR were swapped (15,21). The chimeric ET_BR with C-tail of ET_AR was capable of recycling like wild-type ET_AR, whereas the chimeric ET_AR with C-tail of ET_BR behaved like wild-type ET_BR (15,21). However, the detailed mechanism for the different fates of ET_AR and ET_BR is at present totally unknown.

We have recently shown that ET_BR is ubiquitinated more abundantly than ET_AR in the absence of agonist stimulation (22). To get insights into the mechanisms for different fates of these two receptors, we decided to examine agonist-induced ubiquitination of ET_AR and ET_BR and to analyze the role of ubiquitination in receptor trafficking.

In this study, we show that 1) the different fates of ET_AR and ET_BR are mainly due to agonist-induced ubiquitination of ET_BR but not ET_AR, which occurs on the cell membrane, 2) ubiquitination of ET_BR switches intracellular trafficking of the receptor after agonist-induced internalization, from recycling back to the plasma membrane to lysosomal targeting for degradation, causing a decrease in cell surface levels of the receptor, 3) ubiquitination of the receptor and

consequent decrease in its cell surface levels induce quenching of ET_BR-mediated responses such as ERK phosphorylation and an increase in the intracellular Ca^{2+} concentration ($[Ca^{2+}]_i$) to repetitive agonist stimulation, and 4) ubiquitination at either one of five lysine residues except lysine^{411} in the distal end of C-tail of ET_BR is sufficient for a switch of the intracellular trafficking.

EXPERIMENTAL PROCEDURES

Reagents and Antibodies—The following reagents and antibodies were used: synthetic human ET-1 (Peptide Institute); probenecid and (Sigma-Aldrich); fura-2/acetoxymethyl ester (fura-2/AM) and pluronic F-127 (Dojindo Laboratories); cycloheximide and N-ethylmaleimide (Calbiochem); EZ-Link™ Sulfo-NHS-SS-Biotin and streptavidin agarose resin (Thermo Fisher Scientific); siGENOME® SMARTpool β-arrestin-1 (M-011971-01), siGENOME® SMARTpool β-arrestin-2 (M-007292-00) and siGENOME® Control pool Non-Targeting#1 (D-001206-13-05) (Thermo Scientific Dharmacon®); mouse monoclonal anti-HA epitope tag antibody and Alxa488-conjugated mouse monoclonal anti-HA antibody (Covance); rabbit polyclonal anti-myc epitope tag antibody (Millipore); rabbit polyclonal anti-phospho-ERK1/2 (Thr202/Tyr204) antibody, rabbit polyclonal anti-ERK1/2 antibody and normal rabbit IgG (Cell Signaling Technology); mouse monoclonal anti-GAPDH antibody, mouse monoclonal anti-ubiquitin antibody (P4D1), mouse monoclonal β-arrestin-2 antibody (H-9) (Santa Cruz Biotechnology); rabbit monoclonal anti-β-arrestin-1 antibody and rabbit monoclonal anti-Endothelin B receptor (anti-ET_BR) antibody (abcam); goat polyclonal anti-mouse IgG conjugated to HRP, goat polyclonal anti-rabbit IgG conjugated to HRP and light chain specific mouse monoclonal anti-rabbit IgG conjugated to HRP (Jackson ImmunoResearch Laboratories).

Cell Culture and Transfection—Human embryonic kidney 293T (HEK293T) cells were grown in DMEM supplemented with 10% FBS, 100 units/ml penicillin and 100 μg/ml streptomycin at 37°C in humidified atmosphere containing 5% CO_2. Human pulmonary artery smooth muscle cells (HPASMC) were grown in DMEM supplemented with 20% FBS, 100 units/ml penicillin and 100 μg/ml streptomycin at 37°C in humidified atmosphere containing 5% CO_2. For transfection of plasmid and/or siRNA, Lipofectamine® 2000 reagent (Invitrogen) was used according to the manufacturer's instructions.

Generation of Stable Cell Lines—HEK293T cells stably expressing wild type or mutant N-terminally HA-tagged ETRs, and HEK293T cells stably expressing myc-ubiquitin were generated by retroviral gene transfer as described previously (23,24). The positive cells were selected in DMEM containing 2 μg/ml puromycin for a week, and individual lines were tested by Western blot using an anti-HA antibody. Mutagenesis was performed using KOD-Plus-Mutagenesis Kit (Toyobo) according to the manufacturer's instructions. All of the constructs were verified by DNA sequencing.

Western Blot—The proteins were separated by SDS-PAGE and electrotransferred to a polyvinylidene fluoride membrane (Millipore) with an electroblotter. After transfer, the membranes were washed three times with TBST (10 mM Tris-HCl (pH 8.0), 100 mM NaCl, and 0.1% Tween-20) followed by blocking (2% non-fat dry milk in TBST) of nonspecific binding for 1 h at room temperature. The membranes were incubated with specific antibodies as a primary antibody at 4°C overnight. The primary antibody was detected with a secondary antibody conjugated with HRP. The protein-antibody complex was detected by enhanced chemiluminescence Western blot reagent (Thermo Fisher Scientific). The membranes were exposed to Amersham Hyperfilm™ ECL (GE Healthcare) and the signals were quantified with Image J1.37 software (National Institutes of Health).

Ubiquitination Assay—The HEK293T cells stably expressing wild type or mutant HA-ETRs were transiently transfected with expression vector encoding myc-tagged ubiquitin (myc-ub). Two days after transfection, the cells were incubated with or without ET-1 (30 nM), and lysed using lysis buffer (150 mM NaCl, 1.5 mM $MgCl_2$, 50 mM Tris-HCl (pH 6.8), 1% NP-40, 0.5% sodium

deoxycholate, 0.1% SDS, 1 mM PMSF, 1 mM Na_3VO_4, 20 mM NaF, 10 μg/ml leupeptin, 10 μg/ml aprotinin, and 10 μg/ml pepstatin) containing 20 mM N-ethylmaleimide to inhibit deubiquitinating enzymes. The cell lysates were centrifuged at 20,000 × g for 20 min at 4ºC. Anti-HA antibody (mouse monoclonal) and protein G-Sepharose (GE Healthcare) were added to the supernatants, and the mixture was incubated with rotation at 4°C overnight. The immunocomplexes were washed four times with washing buffer, 1% NP-40, 0.5% sodium deoxycholate, 0.1% SDS) and then analyzed for ubiquitination of receptors by Western blot using rabbit polyclonal anti-myc antibody and goat polyclonal anti-rabbit IgG antibody conjugated to HRP as primary and secondary antibodies, respectively. Reprobing for immunoprecipitated HA-ETRs was performed using anti-HA antibody and goat polyclonal anti-mouse IgG antibody conjugated to HRP as primary and secondary antibodies.

Ubiquitination assay for endogenous ET_BR in HPASMC was performed in a manner essentially similar to that for exogenously expressed HA-ET_BR in HEK293T cells, except for the following points. For immunoprecipitation of ET_BR, rabbit monoclonal anti-ET_BR antibody instead of anti-HA antibody was added to the supernatants of cell lysates, while Western blot analysis of ubiquitinated ET_BR was performed using mouse monoclonal anti-ubiquitin antibody and goat polyclonal anti-mouse IgG antibody conjugated to HRP as primary and secondary antibodies, respectively. Reprobing for immunoprecipitated endogenous ET_BR was performed using rabbit monoclonal anti-ET_BR antibody and light chain specific mouse monoclonal anti-rabbit IgG antibody conjugated to HRP as primary and secondary antibodies, respectively.

Cell Surface HA-ETR Assay—The cells (2×10^6) expressing wild type or mutant HA-ETRs were incubated with 30 nM ET-1 for the indicated times at 37°C. After washing three times with ice-cold PBS (pH 7.4) and resuspension in PBS, the cells were incubated with rotation with 0.5 mg/ml EZ-Link™ Sulfo-NHS-SS-Biotin at 4°C for 1 h to biotinylate cell surface proteins, and the reaction was quenched by adding 50 mM Tris-HCl (pH 8.0)/PBS followed by two washes with ice-cold PBS. The cells were lysed with lysis buffer and centrifuged at 20,000 × g for 20 min at 4ºC. The supernatants were incubated with streptavidin agarose resin at 4°C for 1.5 h to collect biotinylated proteins. The precipitates were washed four times with washing buffer and biotinylated proteins on the streptavidin agarose resin were eluted by adding SDS sample buffer (62.5 mM Tris-HCl (pH 6.8), 10% glycerol, 5% 2-mercaptoethanol, 2.5% SDS, 0.1% bromophenol blue). The resulting supernatant was subjected to Western blot analysis to detect HA-ETRs, which had been on the cell surface after ET-1 stimulation.

Analysis of intracellular trafficking by confocal microscopy—To determine intracellular trafficking pathways for ETRs, we analyzed co-localization of ETRs with either Rab7 or Rab11 as a marker for late endosome/lysosome or recycling endosome, respectively. For this purpose, HEK293T cells were plated on a collagen-coated 35-mm diameter glass base dish (Iwaki, Japan) at a density of 3×10^5 cells per dish. The cells were transiently transfected with either of expression vectors for C-terminally GFP-tagged WT ET_AR (ET_AR-GFP), ET_BR WT-GFP and ET_BR 5KR-GFP, along with either C-terminally tdTomato-tagged Rab7 (Rab7-tdTomato) or Rab11-tdTomato. Twenty four hours after transfection, the cells were incubated with or without ET-1 for 30 min, and fixed in 4% paraformaldehyde for 15 minutes at room temperature. Images were captured by confocal laser microscopy (FV10i, Olympus) and analyzed quantitatively using MetaMorph software (Universal Imaging, West Chester, PA). Namely, vesicles positive for GFP signal or tdTomato signal within each cell were defined based on their intensity and diameter, and subsequently, the number of vesicles within each cell which showed signals for either GFP, tdTomato or both was counted. The extent of co-localization of receptors with Rab proteins was represented as a percentage of the number of vesicles showing both signals to total number of vesicles showing GFP signal alone. Results were obtained from three independent experiments, with 10-13 cells being analyzed in each experiment.

Analysis of internalization of ETRs by confocal microscopy—HA-ET_BR-expressing cells were washed and incubated with Alexa488-conjugated anti-HA antibody for 1 h at 4ºC in serum free DMEM. After washing twice with PBS, the cells were incubated with vehicle or 30 nM ET-1 for 30 min at 37ºC, washed with PBS and fixed with 4% paraformaldehyde. Images were captured by confocal laser microscopy (FV10i, Olympus). Using MetaMorph software, measurements were made in single cells by selecting a region encompassing the entire plasma membrane (defined as total cell region) and then selecting a region just inside the plasma membrane (1.6 μm inside the total cell region; defined as cell inside region). The difference between these two regions was defined as cell membrane region. Fluorescence intensity in total cell region and cell inside region was measured, and fluorescence intensity in cell membrane region was calculated based on fluorescence intensity in these two regions. For estimation of the amount of the internalized receptors, the ratio of the fluorescence intensity in cell membrane region to that in total cell region was determined.

Measurement of the intracellular Ca^{2+} concentration ($[Ca^{2+}]_i$)—$[Ca^{2+}]_i$ was measured as described previously (25,26). HEK293T cells expressing wild type or mutant HA-ET_BRs were incubated in culture medium containing with 4 μM fura-2/AM, 2.5 mM probenecid and 0.04% pluronic F-127 at 37°C for 60 min under reduced light. After washing, the cells were suspended in Ca^{2+}-free Krebs-HEPES solution (140 mM NaCl, 3 mM KCl, 1 mM $MgCl_2$, 11 mM D-(+)-glucose, 10 mM HEPES; adjusted to pH 7.3 with NaOH) at 4×10^5 cells/ml, and stored at 4°C under reduced light. Immediately before $[Ca^{2+}]_i$ measurement, $CaCl_2$ was added to 0.5-ml aliquot of the cell suspension at the final concentration of 2 mM. $[Ca^{2+}]_i$ was measured at 30°C using a CAF-110 spectrophotometer (JASCO) with excitation wavelengths of 340 and 380 nm and an emission wavelength of 500 nm. Data were collected and analyzed using MacLab/8s and Chart (v. 3.5) software (ADInstruments Japan).

Data Analysis—All data were presented as mean ± S.E.M. The significance of the difference between mean values was evaluated with GraphPad PRISM™ (version 3.00, GraphPad Software Inc) by Student's unpaired *t*-test. A *P* value less than 0.05 was considered to indicate statistically significant differences.

RESULTS

ET_BR but not ET_AR is ubiquitinated in C-tail in response to ET-1 stimulation—To evaluate possible ubiquitin modification of the ETRs, we generated HEK293T cells stably expressing either N-terminally HA-tagged ET_AR or ET_BR (referred to as HA-ET_AR or HA-ET_BR, respectively). The cells were transiently transfected with expression vector encoding myc-ubiquitin (myc-ub), stimulated with ET-1 for the indicated times and lysed. HA-ET_AR or HA-ET_BR was immunoprecipitated, and the extent of receptor ubiquitination was determined by Western blot (Fig. 1*A*). Before stimulation with ET-1 (at 0 min), a broad band larger than 80 kDa representing ubiquitinated receptor was observed for HA-ET_BR, but essentially no signal was observed for HA-ET_AR. After stimulation with 30 nM ET-1, no detectable ubiquitination of HA-ET_AR was observed. In sharp contrast, ubiquitination of HA-ET_BR was augmented within 5 min after ET-1 stimulation and lasted, at least, for 20 min (Fig. 1, *A* and *B*). To confirm the relevance of our findings on exogenously expressed receptors in HEK293T cells, we investigated ET-1-induced ubiquitination of endogenously expressed ET_BR in human pulmonary artery smooth muscle cells (HPASMC), and obtained essentially similar results (Fig. 1, *C* and *D*).

β-Arrestins have been shown to function as adaptors for ubiquitination of GPCRs such as β_2-adrenergic receptor (β_2-AR) (27,28), while both ETRs are known to recruit β-arrestins (18,21). Therefore, we examined a role of β-arrestins in

ubiquitination of ET_BR. Knockdown of β-arrestin1 and β-arrestin2 was without effect on basal and ET-1-induced ubiquitination of ET_BR, demonstrating that β-arrestins play no significant role in ubiquitination of ET_BR (Fig. 2).

In order to determine the role of ubiquitination in the regulation of ET_BR trafficking, we constructed mutant ET_BR, which

would not be ubiqutinated. ET_BR has 16 lysine residues in the cytoplasmic region; 8 lysine residues in C-tail (Fig. 3*A*) and 8 other lysine residues in the cytoplasmic loops. Because recent studies have indicated that C-tail might be a major site of ubiquitination in GPCRs (29-32), we first replaced 8 lysine residues in C-tail with arginine (designated HA-ET_BR 8KR). In contrast with wild-type HA-ET_BR, the mutant receptor was found to be not ubiquitinated in an agonist-dependent manner (Fig. 3*B*), suggesting that lysine residues in C-tail are major sites of ubiquitination in ET_BR.

Previously, we demonstrated that ET_BR is palmitoylated at the cysteine cluster of C-tail, and anchored to the plasma membrane (Fig. 3*A*) (9), generating a small loop structure between the 7th transmembrane domain and the palmitoylation sites (Fig. 3*A*). The amino acid sequences of the loop structure are very similar between ET_AR and ET_BR (84% identical) (15), whereas the sequence homology of the region distal to palmitoylation sites is relatively low (26% identical), suggesting the possibility that lysine residues in the region distal to palmitoylation sites in C-tail of ET_BR are the targets for ubiquitination. Therefore, we generated another ET_BR mutant in which 5 lysine residues (K411, K417, K422, K424 and K438) distal to the palmitoylation sites in C-tail were replaced with arginine (designated HA-ET_BR 5KR). As shown in Fig. 3*C*, HA-ET_BR 5KR was not ubiquitinated in an agonist-dependent manner, suggesting that lysine residues distal to the palmitoylation sites are major targets for ubiquitination of ET_BR.

Receptor ubiquitination is involved in ET-1-induced ET_BR internalization—To get insights into the functional significance of ETR ubiquitination, receptor internalization was examined using biotin-streptavidin system to measure the amount of cell surface receptor. The level of cell surface HA-ET_BR rapidly decreased following ET-1 stimulation with a half-life of about 15 min (Fig. 4, *A* and *B*). The level of cell surface HA-ET_AR decreased similarly with HA-ET_BR up to 10 min, but thereafter, it remained almost unchanged (Fig. 4, *A* and *B*). Notably, HA-ET_BR 5KR, the mutant which was not ubiquitinated, disappeared from the cell surface at the rate similar to that of HA-ET_BR WT up to 10 min, but thereafter, at a far slower rate (Fig. 4, *C* and *D*): the time course of disappearance was similar to that of HA-ET_AR (Fig. 4, *B* and *D*).

Next, we attempted to confirm slower internalization of HA-ET_BR 5KR in comparison with that of HA-ET_BR WT using confocal microscopy. Before stimulation with ET-1, major part of HA-ET_BR WT and HA-ET_BR 5KR was present on the cell membrane (Fig. 5, *A*, *upper panels*; Fig. 5, *B*, *left panel*). Thirty minutes after stimulation with ET-1, most of both receptors were internalized, and the number of the receptors remaining on the cell membrane became smaller. Quantitative analysis showed that before ET-1 stimulation, the ratio of cell membrane fluorescence intensity to total cell fluorescence intensity was comparable between cells expressing HA-ET_BR WT and HA-ET_BR 5KR, but that after 30 min-stimulation with ET-1, it was twice as large in cells expressing HA-ET_BR 5KR as that in cells expressing HA-ET_BR WT (Fig. 5, *A*, *lower panels;* Fig. 5, *B*, *right panel*).

Receptor ubiquitination is involved in ET-1-induced ET_BR degradation—We next investigated the role of ubiquitination in ET-1-induced receptor degradation. For this purpose, we determined the disappearance rate of total ETRs in the whole cells after ET-1 stimulation in the presence of a protein synthesis inhibitor, cycloheximide (CHX). In the presence of CHX, the level of total HA-ET_BR decreased with time after ET-1 stimulation, whereas that of total HA-ET_AR was almost unchanged, at least, for 30 min (Fig. 6, *A* and *B*). The disappearance rate of non-ubiquitinated HA-ET_BR 5KR was slower than HA-ET_BR WT (Fig. 6, *C* and *D*) and comparable to that of HA-ET_AR (Fig. 6, *B* and *D*). These results suggest that receptor ubiquitination accelerates ET_BR degradation.

Time course for recovery of cell surface levels of HA-ET_BR WT and HA-ET_BR 5KR following ET-1 stimulation—Toward further understanding of cellular dynamics of HA-ET_BR and HA-ET_BR 5KR, we examined the time course for recovery of cell surface levels of these receptors following ET-1 stimulation. For this purpose, after 30-min stimulation with ET-1, the cells stably expressing

HA-ET_BR WT and HA-ET_BR 5KR were washed two times with ET-1-free medium, cultured for the indicated times and lysed for quantification of cell surface levels of HA-ET_BR WT and HA-ET_BR 5KR by biotinylation assay. After 30-min stimulation with ET-1, cell surface levels of HA-ET_BR WT and HA-ET_BR 5KR were reduced to approximately 30% and 70%, respectively, of control values before stimulation, remained constant up to 2 h and thereafter, began to increase: the level of HA-ET_BR 5KR was recovered to the control level around 4 h, while recovery for the level of HA-ET_BR WT was not complete even 8 h after stimulation (Fig. 7).

ET_BR is ubiquitinated on the cell membrane—We asked whether the ET-1-induced ET_BR ubiquitination occurs, before or after internalization. For that purpose, we overexpressed FLAG-tagged dominant-negative mutant of rat dynamin (DN-dynamin), to inhibit ET_BR internalization (21), and examined its effect on ET_BR ubiquitination. In control cells transfected with empty vector alone, cell surface HA-ET_BR rapidly decreased following ET-1 stimulation (Fig. 8*A*, top panel). In contrast, in cells transfected with DN-dynamin, the disappearance rate of cell surface HA-ET_BR became markedly slower (Fig. 8*A*, top panel), indicating that internalization of cell surface HA-ET_BR was inhibited by DN-dynamin.

Notably, inhibition of internalization by DN-dynamin did not affect ET_BR ubiquitination induced by ET-1 stimulation (Fig. 8, *B* and *C*), indicating that ET_BR is ubiquitinated before internalization, probably on the cell membrane.

Confocal microscopic study of intracellular trafficking of ET_AR, ET_BR or ET_BR 5KR—The apparent rate of receptor internalization in the present study reflects the sum of the rate of receptor endocytosis and the rate of receptor recycling to plasma membrane. Therefore, the slower disappearance of HA-ET_BR 5KR from cell surface following ET-1 stimulation could result from either a decrease in the rate of receptor endocytosis process itself or an increase in receptor recycling to plasma membrane. To differentiate these two possibilities, we analyzed intracellular trafficking pathways of HA-ET_AR, HA-ET_BR WT and HA-ET_BR 5KR using confocal microscopy. For this purpose, we examined co-localization of these receptors with Rab7, a marker for late endosome/lysosome, and Rab11, a marker for recycling endosome (33,34). In one series of experiment, either one of ET_AR-GFP, ET_BR-GFP and ET_BR 5KR-GFP was transiently transfected into HEK293T cells along with Rab7-tdTomato (Fig. 9, *A* and *C*), while in the other series, either one of the receptors was transiently transfected with Rab11-tdTomato (Fig. 9, *B* and *D*). In the absence of ET-1, most of these receptors were localized to the plasma membrane. After 30-min stimulation with ET-1, most of ET_AR-GFP, ET_BR-GFP and ET_BR 5KR-GFP were internalized to the intracellular vesicular structures. ET_AR-GFP was rarely co-localized with Rab7-tdTomato, whereas ET_BR WT-GFP was frequently co-localized with Rab7-tdTomato (Fig. 9, *A* and *C*). Notably, ET_BR 5KR-GFP showed rare co-localization with Rab7-tdTomato, like ET_AR-GFP (Fig. 9, *A* and *C*). Conversely, ET_AR-GFP and ET_BR 5KR-GFP were frequently co-localized with Rab11-tdTomato (Fig. 9, *B* and *D*), whereas ET_BR WT-GFP was rarely co-localized with it (Fig. 9, *B* and *D*). These data clearly demonstrate that after agonist stimulation, ET_AR and non-ubiquitinated ET_BR mutant (5KR) are mainly on the recycling pathway, whereas ET_BR is mainly targeted to lysosome for degradation, and hence, that the slower rate of apparent internalization for ET_BR 5KR at the later phase after ET-1 stimulation is mainly due to recycling to plasma membrane of the receptor.

Functional significance of ET_BR ubiquitination in cellular signaling—To clarify how receptor ubiquitination affects ET_BR-mediated intracellular signaling, we examined ERK phosphorylation and an increase in $[Ca^{2+}]_i$ in cells stably expressing HA-ET_BR WT or HA-ET_BR 5KR in response to two successive stimulation with ET-1. For this purpose, the cells were first stimulated for 30 min with 30 nM ET-1, and they were washed two times with culture medium to remove ET-1: after incubation in fresh medium for 15 min for equilibration, the cells were again stimulated with 30 nM ET-1. In response to the 1st stimulation, ERK phosphorylation levels were increased in cells expressing HA-ET_BR WT or HA-ET_BR 5KR,

and the increase was comparable to each other (Fig. 10, *A* and *B*). Notably, ERK phosphorylation levels in response to the 2nd stimulation became smaller compared to the 1st responses in both types of cells, but the levels were 2-3 times larger in cells expressing HA-ET_BR 5KR than those in cells expressing HA-ET_BR WT (Fig. 10, *A* and *B*). The increase in $[Ca^{2+}]_i$ induced by the first ET-1 stimulation in HA-ET_BR 5KR-expressing cells was similar to that in HA-ET_BR WT-expressing cells (Fig. 10*C*, left panel), but the increase by the second stimulation was about 60% larger than that in HA-ET_BR WT-expressing cells (Fig. 10*C*, right panel). Taking into consideration that the 2nd stimulation was given during the time when changes in cell surface levels of HA-ET_BR WT and HA-ET_BR 5KR following the 1st stimulation are maintained at about 30% and 70% of the values before the 1st stimulation, respectively, these results strongly demonstrate that larger responses to the 2nd stimulation for HA-ET_BR 5KR are due mainly to higher levels of cell surface HA-ET_BR 5KR following the 1st stimulation, resulting from a switch of intracellular trafficking from lysosomal targeting to recycling to plasma membrane. However, considering that ERK phosphorylation and an increase in $[Ca^{2+}]_i$ induced by the second ET-1 stimulation are significantly smaller than the responses expected from cell surface levels of the receptors, it is likely that desensitization mechanisms other than reduced levels of receptors are involved in the reduced responses to the second ET-1 stimulation.

Ubiquitination of either one lysine residue is sufficient for ET-1-induced ET_BR internalization—We asked which lysine residue(s) in C-tail was responsible for ET-1-induced ubiquitination and lysosomal targeting of ET_BR. To clarify this point, we generated a series of ET_BR mutants in which either one of 5 arginine residues (R411, R417, R422, R424 and R438) in C-tail of HA-ET_BR 5KR was reverted to the original lysine (referred to as HA-ET_BR 4KR-411K, 417K, 422K, 424K or 438K, respectively), and examined the ET-1-induced ubiquitination of these mutants. In response to ET-1 stimulation, all of these mutant ET_BRs were ubiquitinated to the level comparable to that of HA-ET_BR WT (Fig. 11, *A* and *B*), suggesting that either one of 5 lysine residues in C-tail of ET_BR WT can be a site of ubiquitination, and also that ET_BR WT is ubiquitinated at only one lysine residue.

We next examined ET-1-induced internalization of these HA-ET_BR 4KR mutants. The disappearance rate of all these mutants except HA-ET_BR 4KR-411K from the cell surface was recovered to that of HA-ET_BR WT: the disappearance rate of HA-ET_BR 4KR-411K remained low, and was similar to that of non-ubiquitinated mutant, HA-ET_BR 5KR (Fig. 11*C*). We wondered whether the dissociation between ubiquitination and internalization of HA-ET_BR 4KR 411K could be due to difference of assay conditions, i.e., the absence or presence of overexpression of myc-ub. Therefore, internalization of the receptor was analyzed after overexpression of myc-ub. Overexpression of myc-ub did not affect the disappearance rate of HA-ET_BR 4KR 411K from the cell surface compared to the rate in the absence of overexpression of myc-ub (data not shown). These data suggest that ubiquitination of any one lysine residue in C-tail, except for $lysine^{411}$ is sufficient for ET-1-induced ET_BR internalization.

We also examined the ET-1-induced degradation rates of HA-ET_BR 4KR mutants, which were indexed by the ET-1-induced decrease in whole cell levels of wild type or mutant HA-ET_BRs during 30 min after treatment with CHX, a protein synthesis inhibitor. As described in Fig. 6, *B* and *D*, in the presence of CHX, ET-1 stimulation for 30 min decreased the whole cell level of wild type HA-ET_BR to 65% of the control value without the stimulation, whereas it had little effect on the whole cell level of non-ubiquitinated mutant, HA-ET_BR 5KR (Fig. 11*D*). In response to ET-1, the whole cell levels of all HA-ET_BR 4KR mutants except for 4KR-411K decreased to the extent comparable to those of wild type HA-ET_BR, whereas the level of HA-ET_BR 4KR-411K was virtually unchanged (Fig. 11*D*). Overexpression of myc-ub did not affect the ET-1-induced degradation rate of HA-ET_BR 4KR 411K (data not shown). These results indicate that ubiquitination of either one of 5 lysine residues except for $lysine^{411}$ in C-tail of ET_BR is

sufficient for ET-1-induced ET_BR degradation.

Finally, we examined ERK phosphorylation in cells stably expressing HA-ET_BR 4KR in response to two successive stimulation with ET-1. An increase in ERK phosphorylation in response to the 1st stimulation was similar between HA-ET_BR WT and HA-ET_BR 4KR mutant (Fig. 12, *A* and data not shown). In accordance with the recovery of receptor internalization and degradation rates, ERK phosphorylation response to the 2nd stimulation was recovered in cells expressing either one of HA-ET_BR 4KR mutants except for HA-ET_BR 4KR-411K to the level in cells expressing HA-ET_BR WT (Fig. 12, *B* and, data not shown), whereas the response in cells expressing HA-ET_BR 4KR-411K remained larger than that in cells expressing HA-ET_BR WT.

DISCUSSION

Two types of receptors for ET-1 such as ET_AR and ET_BR closely resemble each other, but after stimulation with their agonist, they are well-known to follow totally different intracellular trafficking pathways (14,15). That is, after agonist-induced endocytosis, ET_AR is mainly recycled back to the plasma membrane, whereas ET_BR is targeted to lysosome for degradation (14,18). In the present study, we have demonstrated that 1) the different fates of ET_AR and ET_BR are mainly due to agonist-induced ubiquitination of ET_BR but not ET_AR, which occurs on the cell membrane, 2) ubiquitination of ET_BR switches intracellular trafficking of the receptor after agonist-induced internalization, from recycling back to the plasma membrane to targeting to lysosome for degradation, causing a decrease in cell surface levels of the receptor, 3) ubiquitination of the receptor and consequent decrease in its cell surface levels induce quenching of ET_BR-mediated responses such as ERK phosphorylation and an increase in $[Ca^{2+}]_i$ to repetitive agonist stimulation, and 4) ubiquitination at either one of five lysine residues except $lysine^{411}$ in the distal end of C-tail of ET_BR is sufficient for a switch of the intracellular trafficking.

ET_BR but not ET_AR, expressed endogenously in cell lines (HPASMC) and exogenously in HEK293T cells, was specifically ubiquitinated in an agonist-dependent manner, although both receptors possessed several lysine residues as potential ubiquitination sites. Wild-type ET_BR has total 16 lysine residues in the cytoplasmic region as potential ubiquitination sites; 8 lysine residues in the cytoplasmic loops and 8 lysine residues in C-tail. In C-tail, 3 lysine residues are present between the 7th transmembrane domain and palmitoylation sites, while 5 lysine residues are present between the palmitoylation sites and C-tail end (distal C-tail) (Fig. 3*A*). Using mutant receptors named HA-ET_BR 8KR and HA-ET_BR 5KR (in which lysine residues in the whole C-tail and distal C-tail were replaced with arginine, respectively), it was clearly shown that among these 16 potential ubiquitination sites of ET_BR, it is the 5 lysine residues in distal C-tail that are critical for agonist-induced ubiquitination of ET_BR. Conversely, using another series of mutant receptors named ET_BR 4KR in which either one of 5 arginine residues in HA-ET_BR 5KR was reverted to the original lysine, it was shown that wild type ET_BR was ubiquitinated at either one of 5 lysine residues in its C-tail, and that any single lysine residue in distal C-tail of ET_BR except $lysine^{411}$ can function as a ubiquitination site. However, it is unknown whether a preferable ubiquitination site is present and, if present, which lysine residue is the most preferable for ubiquitination. Furthermore, the ubiquitination of ET_BR was found to occur on the cell membrane, according to the experiments with dominant-negative dynamin. This result is consistent with the previous report on μ-opioid receptor (MOR) (35). The reason for lack of ET_AR ubiquitination is at present unknown, although ET_AR has 3 lysine residues as potential ubiquitination sites in the distal C-tail. This difference could be due to that ET_AR is not a good substrate for any E3 ligase.

It is well-known that β-arrestins function as adaptors for ubiquitination of GPCRs such as β_2-AR (27,28) and also that both ET_AR and ET_BR recruit β-arrestins upon agonist stimulation (18,21). However, it is unlikely that β-arrestins are involved in ubiquitination of ET_BR, based on the result that knockdown of both β-arrestin-1 and β-arrestin-2 has little effect on ET-1-induced ubiquitination of the receptor. These results demonstrate that E3 ligase for ET_BR may not

require adaptor proteins for its recruitment to the receptor, or that it may use other adaptor proteins than β-arrestins.

Ubiquitination of ET_BR switches intracellular trafficking of the receptor after agonist-induced endocytosis, from recycling back to the plasma membrane to targeting to lysosome for degradation, causing a decrease in cell surface levels of ET_BR. That is, ubiquitinated ET_BR WT was targeted to lysosome for degradation, judging from ET-1-induced decrease in total amount of the receptor following protein synthesis inhibition by CHX and by dominant localization of ET_BR WT to late endosomes/lysosomes following ET-1 stimulation. In contrast, non-ubiquitinated ET_BR mutant (ET_BR 5 KR) was found to be recycled back to plasma membrane, as evidenced by negligible ET-1-induced decrease in total amount of the receptor following protein synthesis inhibition and by dominant localization of the receptor to recycling endosomes following ET-1 stimulation. This pattern of intracellular trafficking for non-ubiquitinated ET_BR mutant is similar to that for ET_AR, which is not ubiquitinated. Furthermore, restoration of any one arginine residue of ET_BR 5KR C-tail to lysine (ET_BR 4KR) normalized receptor ubiquitination and intracellular trafficking to those of ET_BR WT.

It is reported that some membrane proteins including β_2AR and low-density lipoprotein receptor-related protein are recycled to the plasma membrane by trans-acting proteins such as sorting nexin 27 (SNX27) and SNX17, respectively, which interact with C-tail of those membrane proteins (36,37). Therefore, it is possible that such trans-acting proteins are involved in recycling of ET_AR and probably ET_BR 5KR which shows the same receptor kinetics as ET_AR. In the case of wild type ET_BR, lysosomal targeting signal by receptor ubiquitination might overwhelm recycling signal by trans-acting proteins or ubiquitination of ET_BR might simply inhibit the binding of trans-acting proteins to the receptor. The previous report that a C-tail-truncated mutant of ET_AR is neither internalized nor recycled to the plasma membrane (15,21) may support the presence of such trans-acting proteins. Such trans-acting proteins of ET_AR and ET_BR remain to be identified.

The present study clearly shows that ubiquitination at either one of five lysine residue in the distal C-tail of ET_BR except $lysine^{411}$ is sufficient for switching intracellular trafficking of ET_BR from recycling to plasma membrane to lysosomal targeting. However, the reason for which intracellular trafficking of HA-ET_BR 4KR-411K is not recovered in spite of its ability to be ubiquitinated is at present unknown. It might be due to that ubiquitination of HA-ET_BR 4KR at 411K is not an effective signal either for lysosomal targeting or for inhibiting the binding of recycling machinery such as the above-mentioned trans-acting proteins to the receptor.

The present result that ubiquitination promotes degradation of ET_BR is consistent with previous reports for β_2AR, CXCR4, vasopressin V2 receptor (V2R), protease-activated receptor 2 (PAR2), neurokinin-1 receptor (NK_1R), κ-opioid receptor (KOR) and δ-opioid receptor (DOR) (28-31,38-40). On the other hand, there are few reports showing the involvement of ubiquitination in apparent receptor internalization (or the rate of disappearance of cell surface receptors). That is, in the case of β_2AR, CXCR4, V2R, KOR and DOR, ubiquitination has little effect on the rate of apparent receptor internalization, whereas it accelerates internalization of MOR without effect on receptor recycling to plasma membrane. In this context, ubiquitination of ET_BR is unique in that it accelerates the apparent receptor internalization by switching intracellular trafficking from recycling to lysosomal targeting, presumably without effect on internalization process itself. However, it remains to be determined whether ubiquitination of ET_BR directly affects internalization process itself. The reason for different roles of ubiquitination in receptor internalization among ET_BR, MOR and the other GPCRs is at present unknown, but it might depend on difference of E3 ligases to be involved and the consequent properties/sites of ubiquitination. Indeed, a recent study on β_2AR demonstrates that following binding of different ligands (one is isoprenaline [βAR agonist], while the other is carvedilol [βAR antagonist]) to the receptor, different E3 ligases (such as Nedd4 and MARCH2, respectively) are recruited to ubiquitinate different sites of the receptor, causing different regulation of receptor trafficking: that is, ubiquitination of β_2AR by Nedd4 accelerates only

lysosomal targeting of the receptor, whereas that by MARCH2 accelerates both receptor internalization and lysosomal targeting (41).

Regarding the functional significance of agonist-induced ubiquitination of ET_BR, the present study demonstrates that a decrease in cell surface levels of ET_BR, resulting from agonist-induced acceleration of degradation of ubiquitinated ET_BR, is mainly responsible for quenching of ET_BR-mediated intracellular responses such as ERK phosphorylation and an increase in $[Ca^{2+}]_i$ to repetitive agonist stimulation. However, considering that ERK phosphorylation and $[Ca^{2+}]_i$ response induced by the second ET-1 stimulation are significantly smaller than the responses expected from the extent of a decrease in cell surface levels of the receptors, it is likely that receptor desensitization as well as reduced levels of receptors are involved in the reduced responses to the second ET-1 stimulation. The mechanisms for desensitization remain to be determined.

The ET_BR expression level is reported to be elevated in several pathologic conditions such as atherosclerosis, chronic heart failure and pulmonary hypertension (42-45), and it is probable that the elevated ET_BR levels play a critical role in the genesis and/or development of these pathological conditions. In this context, it is important to investigate the molecular mechanism for the elevated receptor levels, especially in terms of disturbed ubiquitination or enhanced deubiquitination in those pathological conditions. Such study might lead to discovery of novel mechanism for genesis and/or development of these pathological conditions and also of novel therapeutic strategy for those pathological conditions.

REFERENCES

1. Yanagisawa, M., Kurihara, H., Kimura, S., Tomobe, Y., Kobayashi, M., Mitsui, Y., Yazaki, Y., Goto, K., and Masaki, T. (1988) A novel potent vasoconstrictor peptide produced by vascular endothelial cells. *Nature* **332**, 411-415
2. Kobayashi, T., Miyauchi, T., Iwasa, S., Sakai, S., Fan, J., Nagata, M., Goto, K., and Watanabe, T. (2000) Corresponding distributions of increased endothelin-B receptor expression and increased endothelin-1 expression in the aorta of apolipoprotein E-deficient mice with advanced atherosclerosis. *Pathol Int* **50**, 929-936
3. Sakai, S., Miyauchi, T., Kobayashi, M., Yamaguchi, I., Goto, K., and Sugishita, Y. (1996) Inhibition of myocardial endothelin pathway improves long-term survival in heart failure. *Nature* **384**, 353-355
4. Giaid, A., Yanagisawa, M., Langleben, D., Michel, R. P., Levy, R., Shennib, H., Kimura, S., Masaki, T., Duguid, W. P., and Stewart, D. J. (1993) Expression of endothelin-1 in the lungs of patients with pulmonary hypertension. *N Engl J Med* **328**, 1732-1739
5. Arai, H., Hori, S., Aramori, I., Ohkubo, H., and Nakanishi, S. (1990) Cloning and expression of a cDNA encoding an endothelin receptor. *Nature* **348**, 730-732
6. Sakurai, T., Yanagisawa, M., Takuwa, Y., Miyazaki, H., Kimura, S., Goto, K., and Masaki, T. (1990) Cloning of a cDNA encoding a non-isopeptide-selective subtype of the endothelin receptor. *Nature* **348**, 732-735
7. Takagi, Y., Ninomiya, H., Sakamoto, A., Miwa, S., and Masaki, T. (1995) Structural basis of G protein specificity of human endothelin receptors. A study with endothelin$_{A/B}$ chimeras. *The Journal of biological chemistry* **270**, 10072-10078
8. Kawanabe, Y., Okamoto, Y., Nozaki, K., Hashimoto, N., Miwa, S., and Masaki, T. (2002) Molecular mechanism for endothelin-1-induced stress-fiber formation: analysis of G proteins using a mutant endothelin$_A$ receptor. *Mol Pharmacol* **61**, 277-284
9. Okamoto, Y., Ninomiya, H., Tanioka, M., Sakamoto, A., Miwa, S., and Masaki, T. (1997) Palmitoylation of human endothelin$_B$. Its critical role in G protein coupling and a differential requirement for the cytoplasmic tail by G protein subtypes. *The Journal of biological chemistry* **272**, 21589-21596
10. Horinouchi, T., Terada, K., Higashi, T., and Miwa, S. Endothelin receptor signaling: new insight into its regulatory mechanisms. *J Pharmacol Sci* **123**, 85-101
11. Fukuroda, T., Fujikawa, T., Ozaki, S., Ishikawa, K., Yano, M., and Nishikibe, M. (1994) Clearance of circulating endothelin-1 by ET_B receptors in rats. *Biochem Biophys Res Commun* **199**, 1461-1465
12. Yanagisawa, M., and Masaki, T. (1989) Endothelin, a novel endothelium-derived peptide. Pharmacological activities, regulation and possible roles in cardiovascular control. *Biochem Pharmacol* **38**, 1877-1883
13. de Nucci, G., Thomas, R., D'Orleans-Juste, P., Antunes, E., Walder, C., Warner, T. D., and Vane, J. R. (1988) Pressor effects of circulating endothelin are limited by its removal in the pulmonary circulation and by the release of prostacyclin and endothelium-derived relaxing factor. *Proc Natl Acad Sci U S A* **85**, 9797-9800
14. Oksche, A., Boese, G., Horstmeyer, A., Furkert, J., Beyermann, M., Bienert, M., and Rosenthal, W. (2000) Late endosomal/lysosomal targeting and lack of recycling of the ligand-occupied endothelin B receptor. *Mol Pharmacol* **57**, 1104-1113
15. Abe, Y., Nakayama, K., Yamanaka, A., Sakurai, T., and Goto, K. (2000) Subtype-specific trafficking of endothelin receptors. *The Journal of biological chemistry* **275**, 8664-8671
16. Sakamoto, A., Yanagisawa, M., Sakurai, T., Takuwa, Y., Yanagisawa, H., and Masaki, T. (1991) Cloning and functional expression of human cDNA for the ET_B endothelin receptor. *Biochem*

Biophys Res Commun **178**, 656-663
17. Sakamoto, A., Yanagisawa, M., Sawamura, T., Enoki, T., Ohtani, T., Sakurai, T., Nakao, K., Toyo-oka, T., and Masaki, T. (1993) Distinct subdomains of human endothelin receptors determine their selectivity to endothelin$_A$-selective antagonist and endothelin$_B$-selective agonists. *The Journal of biological chemistry* **268**, 8547-8553
18. Bremnes, T., Paasche, J. D., Mehlum, A., Sandberg, C., Bremnes, B., and Attramadal, H. (2000) Regulation and intracellular trafficking pathways of the endothelin receptors. *The Journal of biological chemistry* **275**, 17596-17604
19. Whistler, J. L., Enquist, J., Marley, A., Fong, J., Gladher, F., Tsuruda, P., Murray, S. R., and Von Zastrow, M. (2002) Modulation of postendocytic sorting of G protein-coupled receptors. *Science* **297**, 615-620
20. Trejo, J., and Coughlin, S. R. (1999) The cytoplasmic tails of protease-activated receptor-1 and substance P receptor specify sorting to lysosomes versus recycling. *The Journal of biological chemistry* **274**, 2216-2224
21. Paasche, J. D., Attramadal, T., Sandberg, C., Johansen, H. K., and Attramadal, H. (2001) Mechanisms of endothelin receptor subtype-specific targeting to distinct intracellular trafficking pathways. *The Journal of biological chemistry* **276**, 34041-34050
22. Nishimoto, A., Lu, L., Hayashi, M., Nishiya, T., Horinouchi, T., and Miwa, S. (2010) Jab1 regulates levels of endothelin type A and B receptors by promoting ubiquitination and degradation. *Biochem Biophys Res Commun* **391**, 1616-1622
23. Nishiya, T., Matsumoto, K., Maekawa, S., Kajita, E., Horinouchi, T., Fujimuro, M., Ogasawara, K., Uehara, T., and Miwa, S. (2011) Regulation of inducible nitric-oxide synthase by the SPRY domain- and SOCS box-containing proteins. *The Journal of biological chemistry* **286**, 9009-9019
24. Horinouchi, T., Higa, T., Aoyagi, H., Nishiya, T., Terada, K., and Miwa, S. (2012) Adenylate cyclase/cAMP/protein kinase A signaling pathway inhibits endothelin type A receptor-operated Ca^{2+} entry mediated via transient receptor potential canonical 6 channels. *J Pharmacol Exp Ther* **340**, 143-151
25. Horinouchi, T., Nishimoto, A., Nishiya, T., Lu, L., Kajita, E., and Miwa, S. (2007) Endothelin-1 decreases $[Ca^{2+}]_i$ via Na^+/Ca^{2+} exchanger in CHO cells stably expressing endothelin ET_A receptor. *Eur J Pharmacol* **566**, 28-33
26. Horinouchi, T., Higashi, T., Higa, T., Terada, K., Mai, Y., Aoyagi, H., Hatate, C., Nepal, P., Horiguchi, M., Harada, T., and Miwa, S. (2012) Different binding property of STIM1 and its novel splice variant STIM1L to Orai1, TRPC3, and TRPC6 channels. *Biochem Biophys Res Commun* **428**, 252-258
27. Shenoy, S. K., Xiao, K., Venkataramanan, V., Snyder, P. M., Freedman, N. J., and Weissman, A. M. (2008) Nedd4 mediates agonist-dependent ubiquitination, lysosomal targeting, and degradation of the β_2-adrenergic receptor. *The Journal of biological chemistry* **283**, 22166-22176
28. Shenoy, S. K., McDonald, P. H., Kohout, T. A., and Lefkowitz, R. J. (2001) Regulation of receptor fate by ubiquitination of activated β_2-adrenergic receptor and β-arrestin. *Science* **294**, 1307-1313
29. Cottrell, G. S., Padilla, B., Pikios, S., Roosterman, D., Steinhoff, M., Gehringer, D., Grady, E. F., and Bunnett, N. W. (2006) Ubiquitin-dependent down-regulation of the neurokinin-1 receptor. *The Journal of biological chemistry* **281**, 27773-27783
30. Marchese, A., and Benovic, J. L. (2001) Agonist-promoted ubiquitination of the G protein-coupled receptor CXCR4 mediates lysosomal sorting. *The Journal of biological chemistry* **276**, 45509-45512
31. Li, J. G., Haines, D. S., and Liu-Chen, L. Y. (2008) Agonist-promoted Lys63-linked polyubiquitination of the human κ-opioid receptor is involved in receptor down-regulation. *Mol Pharmacol* **73**, 1319-1330
32. Chen, B., Dores, M. R., Grimsey, N., Canto, I., Barker, B. L., and Trejo, J. (2011) Adaptor protein complex-2 (AP-2) and epsin-1 mediate protease-activated receptor-1 internalization via

phosphorylation- and ubiquitination-dependent sorting signals. *The Journal of biological chemistry* **286**, 40760-40770

33. Seachrist, J. L., and Ferguson, S. S. (2003) Regulation of G protein-coupled receptor endocytosis and trafficking by Rab GTPases. *Life sciences* **74**, 225-235
34. Fujioka, Y., Tsuda, M., Nanbo, A., Hattori, T., Sasaki, J., Sasaki, T., Miyazaki, T., and Ohba, Y. (2013) A Ca^{2+}-dependent signalling circuit regulates influenza A virus internalization and infection. *Nature communications* **4**, 2763
35. Henry, A. G., Hislop, J. N., Grove, J., Thorn, K., Marsh, M., and von Zastrow, M. (2012) Regulation of endocytic clathrin dynamics by cargo ubiquitination. *Dev Cell* **23**, 519-532
36. van Kerkhof, P., Lee, J., McCormick, L., Tetrault, E., Lu, W., Schoenfish, M., Oorschot, V., Strous, G. J., Klumperman, J., and Bu, G. (2005) Sorting nexin 17 facilitates LRP recycling in the early endosome. *EMBO J* **24**, 2851-2861
37. Lauffer, B. E., Melero, C., Temkin, P., Lei, C., Hong, W., Kortemme, T., and von Zastrow, M. (2010) SNX27 mediates PDZ-directed sorting from endosomes to the plasma membrane. *J Cell Biol* **190**, 565-574
38. Jacob, C., Cottrell, G. S., Gehringer, D., Schmidlin, F., Grady, E. F., and Bunnett, N. W. (2005) c-Cbl mediates ubiquitination, degradation, and down-regulation of human protease-activated receptor 2. *The Journal of biological chemistry* **280**, 16076-16087
39. Martin, N. P., Lefkowitz, R. J., and Shenoy, S. K. (2003) Regulation of V2 vasopressin receptor degradation by agonist-promoted ubiquitination. *The Journal of biological chemistry* **278**, 45954-45959
40. Hislop, J. N., Henry, A. G., Marchese, A., and von Zastrow, M. (2009) Ubiquitination regulates proteolytic processing of G protein-coupled receptors after their sorting to lysosomes. *The Journal of biological chemistry* **284**, 19361-19370
41. Han, S. O., Xiao, K., Kim, J., Wu, J. H., Wisler, J. W., Nakamura, N., Freedman, N. J., and Shenoy, S. K. (2012) MARCH2 promotes endocytosis and lysosomal sorting of carvedilol-bound β_2-adrenergic receptors. *J Cell Biol* **199**, 817-830
42. Iwasa, S., Fan, J., Shimokama, T., Nagata, M., and Watanabe, T. (1999) Increased immunoreactivity of endothelin-1 and endothelin B receptor in human atherosclerotic lesions. A possible role in atherogenesis. *Atherosclerosis* **146**, 93-100
43. Schneider, M. P., Boesen, E. I., and Pollock, D. M. (2007) Contrasting actions of endothelin ET_A and ET_B receptors in cardiovascular disease. *Annu Rev Pharmacol Toxicol* **47**, 731-759
44. Bohm, F., Ahlborg, G., Johansson, B. L., Hansson, L. O., and Pernow, J. (2002) Combined endothelin receptor blockade evokes enhanced vasodilatation in patients with atherosclerosis. *Arterioscler Thromb Vasc Biol* **22**, 674-679
45. Bohm, F., and Pernow, J. (2007) The importance of endothelin-1 for vascular dysfunction in cardiovascular disease. *Cardiovasc Res* **76**, 8-18

Acknowledgements—We are grateful to Dr. Nagasawa (Gunma university) for kindly providing us with a cDNA for dominant-negative rat dynamin (K44A).

FOOTNOTES

*This work was supported in part by Grant-in-Aids for Scientific Research (B) 24390059 (S.M.), Challenging Exploratory Research 25670123 (S.M.) and Scientific Research (C) 25460326 (K.T.) from the Japan Society for the Promotion of Science (JSPS) and in part by grant from the Smoking Research Foundation of Japan (S.M.) and Suzuken Memorial Foundation (K.T.).

[1]To whom correspondence should be addressed: Department of Cellular Pharmacology, Hokkaido University Graduate School of Medicine, North 15, West 7, Kita-ku, Sapporo 060-8638, Japan. Tel.: +81-11-706-6921; Fax: +81-11-706-7824.
E-mail: smiwa@med.hokudai.ac.jp

[2]The abbreviations used are: ET-1, endothelin-1; ET_AR, endothelin type A receptor; ET_BR, endothelin type B receptor; C-tail, carboxyl terminal tail; GPCR, G protein coupled receptor; fura-2/AM, fura-2/acetoxymethyl ester; HEK293T, human embryonic kidney 293T; HPASMC, human pulmonary artery smooth muscle cells; myc-ub, myc-tagged ubiquitin; β_2AR, β_2-adrenergic receptor; $[Ca^{2+}]_i$, intracellular Ca^{2+} concentration; CHX, cycloheximide; DN-dynamin, FLAG-tagged dominant-negative mutant of rat dynamin; MOR, μ-opioid receptor; SNX27, sorting nexin 27; V2R, vasopressin V2 receptor; PAR2, protease-activated receptor 2; NK_1R, neurokinin-1 receptor; KOR, κ-opioid receptor; DOR, δ-opioid receptor.

FIGURE LEGENDS

FIGURE 1. **ET-1 stimulation induces ubiquitination of ET_BR but not ET_AR.** *A*, HEK293T cells stably expressing HA-ET_AR or HA-ET_BR were transiently transfected with myc-ubiquitin (myc-ub), and stimulated with 30 nM ET-1 for the indicated times. The cell extracts were immunoprecipitated (IP) with anti-HA monoclonal antibody conjugated with protein G-Sepharose, and ubiquitinated receptors were analyzed by immunoblot (IB) with anti-myc polyclonal antibody (top panel). The same blot was reprobed for HA-ET_AR or HA-ET_BR using anti-HA monoclonal antibody (second panel). Western blot analysis of the cell extract for myc-ub (third panel) or GAPDH (bottom panel). Shown was a representative blot from three independent experiments. *B*, The ubiquitin signals in the immunoprecipitates were quantified, normalized to the signals of immunopreciptated HA-ET_BR, and the value after normalization was represented as an fold-increase over the control value at time 0. Each point represents mean ± S.E.M of three independent experiments. *, $P < 0.05$; **, $P < 0.01$ versus time 0. *C*, Human pulmonary artery smooth muscle cells (HPASMC) expressing endogenous ET_BR were stimulated with 30 nM ET-1 for 10 min. The cell extracts were IP with anti-ET_BR antibody conjugated with protein G-Sepharose, and ubiquitinated receptors were analyzed by IB with anti-ubiquitin monoclonal antibody (upper panel). The same blots were analyzed by IB with anti-ET_BR antibody (lower panel). *D*, Control experiment to confirm that IB signal between 50 kDa and 60 kDa reflects ET_BR but not IgG heavy chain used for IP in *C*. Cell lysis buffer (Buffer) and cell extracts of HPASMC (Extract) were incubated with indicated antibodies (α-ET_BR, α-β-arrestin1 or Normal rabbit IgG) conjugated with protein G-Sepharose for IP. The resulting immunoprecipitates were analyzed by IB with anti-ET_BR (α-ET_BR) antibody and light chain specific anti-rabbit IgG conjugated with HRP as primary and secondary antibody, respectively.

FIGURE 2. **Effects of knock-down of β-arrestin1 and β-arrestin2 by siRNA on ubiquitination of ET_BR.** *A*, HEK293T cells stably expressing myc-ubiquitin (myc-ub) were transfected with HA-ET_BR WT in combination with either control siRNA or siRNAs targeting for β-arrestin1 or β-arrestin2. Three days after transfection, the cells were incubated with or without ET-1 for 20 min and ubiquitination of HA-ET_BR was analyzed as described in the legend for Figure 1 (top panel). The same blots were

analyzed by immunoblot (IB) with anti-HA antibody (second panel). Western blot analysis of the cell extracts for myc-ub (third panel), β-arrestin1 (fourth panel), β-arrestin2 (fifth panel) and GAPDH (bottom panel). *B*, The ubiquitin signals in the immunoprecipitates were quantified, normalized to the signals of immunopreciptated HA-ET_BR, and the value after normalization was represented as a percentage of the value in the unstimulated cells transfected with control siRNA. Each bar graph represents mean ± S.E.M of three independent experiments. **, $P < 0.01$ versus the value in the absence of ET-1 stimulation; n.s., not significantly different.

FIGURE 3. **Mutations of lysine residues in the cytoplasmic carboxyl terminal tail (C-tail) abolished ubiquitination of ET_BR.** *A*, Schematic representation of the ET_BR with N-terminal HA epitope tag and amino acid sequence of C-terminal. An arrow indicates a cluster of cysteines which are palmitoylated. The locations of lysine (K) residues that were mutated to arginine in HA-ET_BR 8KR are shown in black. *B and C*, HEK293T cells stably expressing wild type HA-ET_BR (WT), HA-ET_BR 8KR (8KR) (*B*) or HA-ET_BR 5KR (5KR) (*C*) were transiently transfected with myc-ubiquitin (myc-ub), stimulated with 30 nM ET-1 for the indicated times, and ubiquitination of these receptors was analyzed as described in the legend for Figure 1 (top panels). The same blots were analyzed by immunoblot with anti-HA monoclonal antibody (second panels). Western blot analysis of the cell extract for myc-ub (third panels) and GAPDH (bottom panels). Shown were representative blots from three independent experiments.

FIGURE 4. **Receptor ubiquitination is required for agonist-induced internalization of ET_BR.** HEK293T cells stably expressing HA-ET_AR WT or HA-ET_BR WT (*A, B*) and the cells stably expressing HA-ET_BR WT or HA-ET_BR 5KR (*C, D*) were stimulated with 30 nM ET-1 for the indicated times. After the stimulation, cell surface proteins were labeled with biotin, biotinylated proteins in cell lysates were collected using streptavidin resin, and probed for the receptors with anti-HA monoclonal antibody (top panels in *A* & *C*). Western blot analysis of the cell lysates for the receptors (middle panels in *A* & *C*) and GAPDH (bottom panels in *A* & *C*). Shown were representative blots from three independent experiments (*A, C*). The amount of cell surface receptors was quantified, normalized to that of total receptors in cell lysates and the value after normalization at each time was represented as a percentage of the value at 0 min (*B, D*). *, $P < 0.05$; **, $P < 0.01$ versus HA-ET_AR WT (*B*) or HA-ET_BR WT (*D*).

FIGURE 5. **Confocal microscopic analysis of agonist-induced internalization of HA-ET_BR WT and HA-ET_BR 5KR mutant.** HEK293T cells stably expressing HA-ET_BR WT (WT, left panels in *A*) or non-ubiquitinated HA-ET_BR 5KR mutant (5KR, right panels in *A*) were incubated with Alexa488-conjugated anti-HA antibody for 1 h at 4°C to label cell surface receptors. After washout of free antibody, the cells were incubated with vehicle (upper panels in *A*; left panel in *B*) or 30 nM ET-1 (lower panels in *A*; right panel in *B*) for 30 min at 37°C. Subsequently, they were fixed with 4% paraformaldehyde and subjected to image analysis by confocal microscopy (*A*). Quantitative analysis of confocal images was performed using MetaMorph software (*B*). Namely, total cell region and cell membrane region were selected in single cells as described in "Experimental Procedures", fluorescence intensity in these regions was determined and the ratio of the fluorescence intensity in total cell region to that in cell membrane region was calculated. Each bar graph represents mean ± S.E.M. n = 15-17. **, $P < 0.01$ versus HA-ET_BR WT. Scale bar, 10 μm.

FIGURE 6. **Receptor ubiquitination is required for agonist-induced degradation of ET_BR.** HEK293T cells stably expressing HA-ET_AR WT or HA-ET_BR WT (*A, B*) and the cells stably expressing HA-ET_BR WT or HA-ET_BR 5KR (*C, D*) were stimulated with 30 nM ET-1 for the indicated times in the presence of 50 μM cycloheximide (CHX), a protein synthesis inhibitor, and the cell lysates were analyzed by Western blot for the receptors using anti-HA monoclonal antibody (upper panels in *A* & *C*) and for GAPDH (lower panels in *A* & *C*). Shown were representative blots from three independent experiments (*A, C*). The amount of total receptors in cell lysates was quantified, normalized to that of GAPDH and

the value after normalization at each time was represented as a percentage of the value at 0 min (*B, D*). Each point represents mean ± S.E.M of three independent experiments. *, $P < 0.05$; **, $P < 0.01$ versus HA-ET_AR WT (*B*) or HA-ET_BR WT (*D*).

FIGURE 7. **Time course of recovery of cell surface levels for HA-ET_BR WT and HA-ET_BR 5KR following ET-1 stimulation for 30 min.** *A,* HEK293T cells stably expressing HA-ET_BR WT or HA-ET_BR 5KR were stimulated with 30 nM ET-1 for 30 min. After stimulation, the cells were washed with ET-1-free medium and cultured for indicated times. Cell surface receptor levels were analyzed by the biotinylation method as described in the legend for Figure 4. Shown were representative blots from three independent experiments. *B,* Cell surface receptor levels were quantified, normalized to total receptor levels in cell lysates which were quantified by Western blot analysis, and the value after normalization at each time was represented as a percentage of the value before stimulation (the values at -0.5 h). Each point represents mean ± S.E.M of three independent experiments. ##, $P < 0.01$ versus the value at -0.5 h for HA-ET_BR WT; *, $P < 0.05$; **, $P < 0.01$ versus the value at -0.5 h for HA-ET_BR 5KR.

FIGURE 8. **ET_BR is ubiquitinated on the cell membrane in response to ET-1 stimulation.** *A,* Inhibition of internalization of HA-ET_BR WT by dominant-negative dynamin. HEK293T cells stably expressing HA-ET_BR WT were transiently transfected with empty vector (Mock) or FLAG-tagged dominant-negative dynamin (DN-dyn), and the cells were stimulated with 30 nM ET-1 for the indicated times. After the stimulation, cell surface HA-ET_BR WT was detected using the biotinylation method as described in Figure 4 (top panel). Western blot analysis of cell lysates for HA-ET_BR WT (the second panel), GAPDH (the third panel) and the DN-dyn (bottom panel). Shown was a representative blot from three independent experiments. *B* and *C,* Effects of DN-dyn on the ET-1-induced ubiquitination of HA-ET_BR WT. HEK293T cells stably expressing HA-ET_BR WT were transiently transfected with myc-ubiquitin (myc-ub) in combination with either empty vector (Mock) or DN-dyn, and the cells were incubated with or without 30 nM ET-1 for 20 min. The ET-1-induced ubiquitination of HA-ET_BR WT was determined as described in the legend for Figure 1 (top panel). The same blot was reprobed for HA-ET_BR WT using anti-HA monoclonal antibody (the second panel). Western blot analysis of cell lysates for myc-ub (third panel), GAPDH (fourth panel) and DN-dyn (bottom panel). Shown were representative blots from three independent experiments. The amount of ubiquitinated HA-ET_BR WT was quantified, normalized to that of total receptor in IP and the value after normalization was represented as a percentage of the value for the Mock-transfected, unstimulated cells (*C*). Each bar graph represents mean ± S.E.M of three independent experiments. **, $P < 0.01$ versus no stimulation in mock- or DN-dyn-transfected group; n.s., not significantly different.

FIGURE 9. **Co-localization of ET_AR, ET_BR or ET_BR-5KR with Rab-7 (a marker for late endosome/lysosome), or Rab-11 (a marker for recycling endosome).** HEK293T cells were transiently transfected with Rab7-tdTomato (*A, C*) or Rab11-tdTomato (*B, D*) in combination with either ET_AR-GFP, ET_BR WT-GFP or ET_BR 5KR-GFP. One day after transfection, the cells were incubated with vehicle or 30 nM ET-1 for 30 min at 37°C, fixed with 4% paraformaldehyde and images were acquired using confocal microscopy. Panels in the leftmost and middle rows in A or B show subcellular distribution of either of the receptors (green) and Rab7/11 (red), respectively, while panels in the rightmost row show merged images (yellow). Results are representative of images obtained from three independent experiments (*A, B*). Scale bar, 10 μm. Co-localization of endothelin receptors with Rab proteins within cells after incubation with ET-1 for 30 min was quantified and represented as percentages of the number of vesicles showing signals for both GFP and tdTomato against the number of vesicles showing GFP signal alone. From three independent experiments, 10-13 cells were analyzed in each experiment (*C, D*). Each bar graph represents mean ± S.E.M. **, $P < 0.01$ versus HA-ET_BR WT (*C, D*); n.s., not significantly different from HA-ET_AR (*C*); #, $P < 0.05$ versus HA-ET_AR (*D*).

FIGURE 10. **Comparison of ERK phosphorylation and increases in the intracellular Ca^{2+} concentration in cells expressing HA-ET_BR WT or 5KR mutant in response to two successive stimulation with ET-1.** *A* and *B*, ERK phosphorylation in response to the first (left panels) and second ET-1 stimulation (right panels). HEK293T cells expressing HA-ET_BR WT (WT) or HA-ET_BR 5KR (5KR) were first stimulated with 30 nM ET-1 for 30 min at 37°C. After washing two times with fresh culture medium and subsequent equilibration for 15 min, the cells were again stimulated with 30 nM ET-1. At the indicated times after the beginning of the 1st and 2nd stimulation, the cells were lysed and phosphorylated ERK1/2 (p-ERK) (upper panel) and total ERK (lower panel) were analyzed by Western blot (*A*). Shown were representative blots from three independent experiments. The signal for p-ERK was normalized to that of total ERK at each time, and the value after normalization was represented as a fold increase of the value at 0 min after the second stimulation for HA-ET_BR WT (*B*). Each point represents mean ± S.E.M of three independent experiments. *, $P < 0.05$ versus HA-ET_BR WT. *C*, $[Ca^{2+}]_i$ responses induced by the first (left) and second (right) ET-1 stimulation in the cells expressing HA-ET_BR WT or HA-ET_BR 5KR. After the cells had been load with Ca^{2+} indicator fura-2, they were sequentially stimulated with 30 nM ET-1 as described above, and the peak increase in $[Ca^{2+}]_i$ was measured as described in "Experimental Procedures". Each bar graph represents mean ± S.E.M of three independent experiments. **, $P < 0.01$ versus HA-ET_BR WT.

FIGURE 11. **ET-1-induced ubiquitination of either one of 5 lysine residues except $lysine^{411}$ in ET_BR C-tail is sufficient for internalization and degradation of ET_BR.** *A* and *B*, ET-1-induced ubiquitination of HA-ET_BR WT and HA-ET_BR 4KR. HEK293T cells stably expressing HA-ET_BR WT or either one of HA-ET_BR 4KR mutants (4KR-411K, 417K, 422K, 424K, 438K) were transiently transfected with myc-ubiquitin (myc-ub). The cells were incubated with or without 30 nM ET-1 for 20 min, and the ubiquitination of the receptors was analyzed (*A*, top panel) and quantified (*B*) as described in Figure 1. The same blot was reprobed for HA-ET_BR WT using anti-HA monoclonal antibody (*A*, second panel). Western blot analysis of cell lysates for myc-ub (third panel) and GAPDH (*A*, bottom panel). Each bar graph represents mean ± S.E.M of three independent experiments (*B*). *, $P < 0.05$; **, $P < 0.01$ versus no ET-1 stimulation; n.s., not significantly different from HA-ET_BR WT. *C*, ET-1-induced internalization of HA-ET_BR WT, HA-ET_BR 5KR and HA-ET_BR 4KR. HEK293T cells stably expressing HA-ET_BR WT, HA-ET_BR 5KR or HA-ET_BR 4KR were stimulated with 30 nM ET-1 for the indicated times at 37°C. After the stimulation, cell surface receptors were quantified as described in the legend for Figure 4. Each point represents mean ± S.E.M of three independent experiments. *, $P < 0.05$; **, $P < 0.01$ versus HA-ET_BR WT. *D*, ET-1-induced degradation of HA-ET_BR WT, HA-ET_BR 5KR and HA-ET_BR 4KR. HEK293T cells expressing HA-ET_BR WT, HA-ET_BR 5KR or HA-ET_BR 4KR were incubated with or without 30 nM ET-1 at 37°C in the presence 50 μM of CHX. After the incubation, receptor levels in whole cell lysates were quantified as described in the legend for Figure 6 and the value after ET-1 stimulation was represented as a percentage of the value before ET-1 stimulation. Each bar graph represents mean ± S.E.M of three independent experiments. *, $P < 0.05$; **, $P < 0.01$ versus HA-ET_BR WT; n.s., not significantly different from HA-ET_BR WT.

FIGURE 12. **Normalization of the ET-1-induced ERK phosphorylation in the cells expressing HA-ET_BR 4KR-417K but not HA-ET_BR 4KR-411K.** HEK293T cells expressing HA-ET_BR WT (WT) or either one of HA-ET_BR 4KR mutants (411K or 417K) were sequentially stimulated with 30 nM ET-1 for 30 min at 37°C as described in the legend for Figure 10. At the indicated times after the beginning of the 1st (*A*) and 2nd (*B*) stimulation, the cells were lysed, and phosphorylated ERK1/2 (p-ERK) (upper panels in *A* and *B*) and total ERK (lower panels) in whole cell lysates were analyzed by Western blot. Shown were representative blots from three independent experiments. The signal for p-ERK was normalized to that of total ERK at each time, and the value after normalization was represented as a fold increase of the value at 0 min after the second stimulation for HA-ET_BR WT (*C* and *D*). Each point represents mean ± S.E.M of three independent experiments (*C* and *D*). *, $P < 0.05$ versus HA-ET_BR WT.

Figure 1

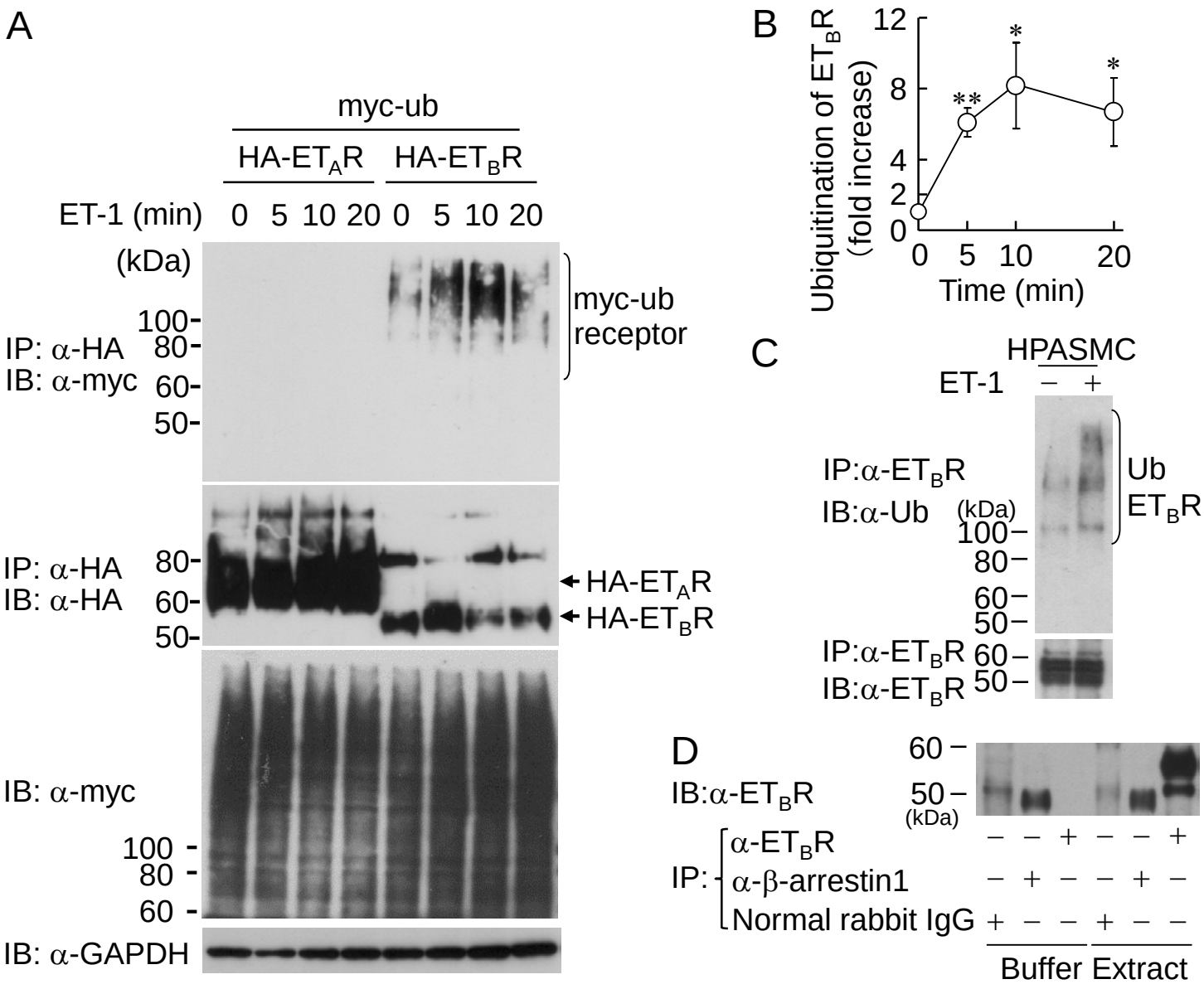
A
myc-ub
HA-ET$_A$R
HA-ET$_B$R
ET-1 (min) 0 5 10 20 0 5 10 20
(kDa)
100
80
60
50
IP: α-HA
IB: α-myc
myc-ub
receptor
IP: α-HA
IB: α-HA
80
60
50
HA-ET$_A$R
HA-ET$_B$R
IB: α-myc
100
80
60
IB: α-GAPDH
B
Ubiquitination of ET$_B$R
(fold increase)
12
8
4
2
0
0 5 10 20
Time (min)
C
HPASMC
ET-1 − +
IP:α-ET$_B$R
IB:α-Ub
(kDa)
100
80
60
50
Ub
ET$_B$R
IP:α-ET$_B$R
IB:α-ET$_B$R
60
50
D
IB:α-ET$_B$R
60
50
(kDa)
IP:
α-ET$_B$R
α-β-arrestin1
Normal rabbit IgG
− − + − − +
− + − − + −
+ − − + − −
Buffer Extract

Figure 2

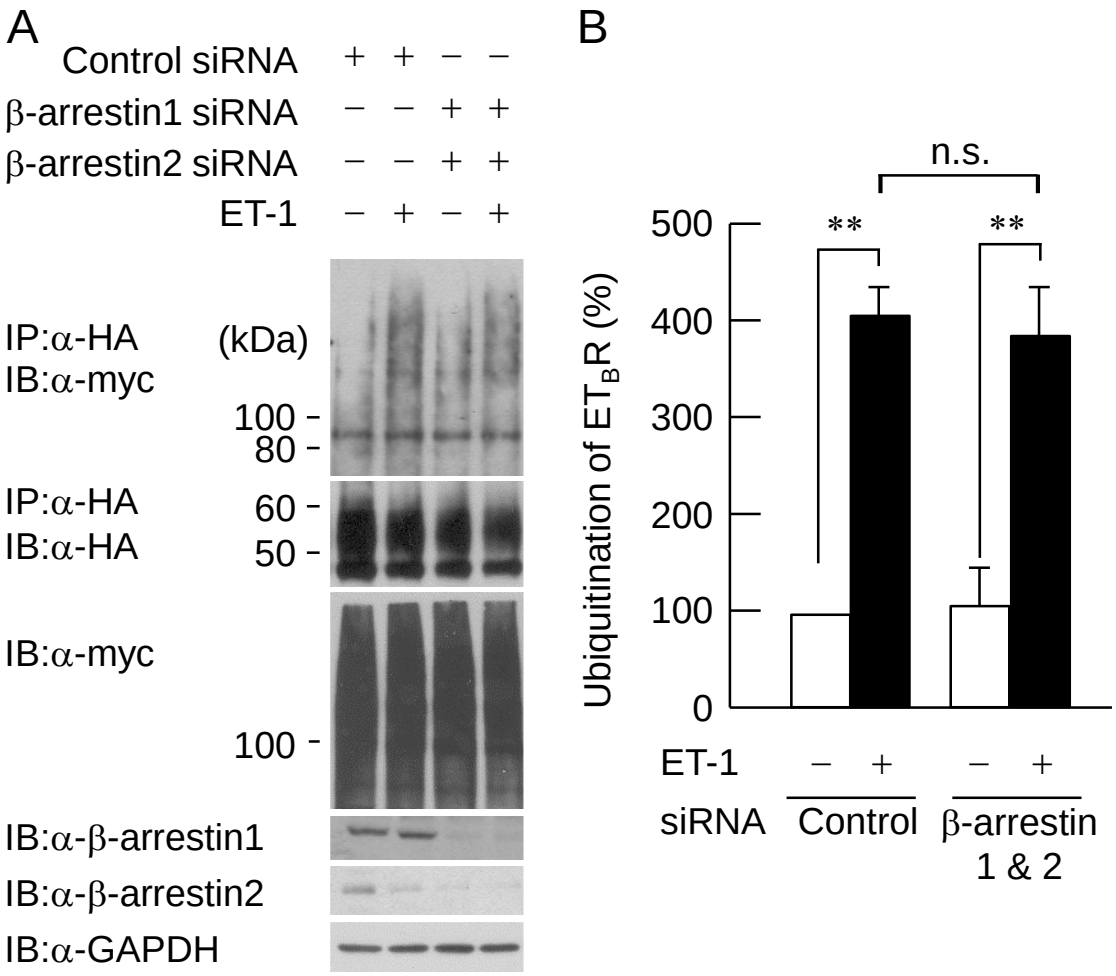
A
Control siRNA + + − −
β-arrestin1 siRNA − − + +
β-arrestin2 siRNA − − + +
ET-1 − + − +
IP:α-HA
IB:α-myc
(kDa)
100
80
IP:α-HA
IB:α-HA
60
50
IB:α-myc
100
IB:α-β-arrestin1
IB:α-β-arrestin2
IB:α-GAPDH
B
n.s.
**
**
Ubiquitination of ETBR (%)
500
400
300
200
100
0
ET-1 − + − +
siRNA Control β-arrestin 1 & 2

Figure 3

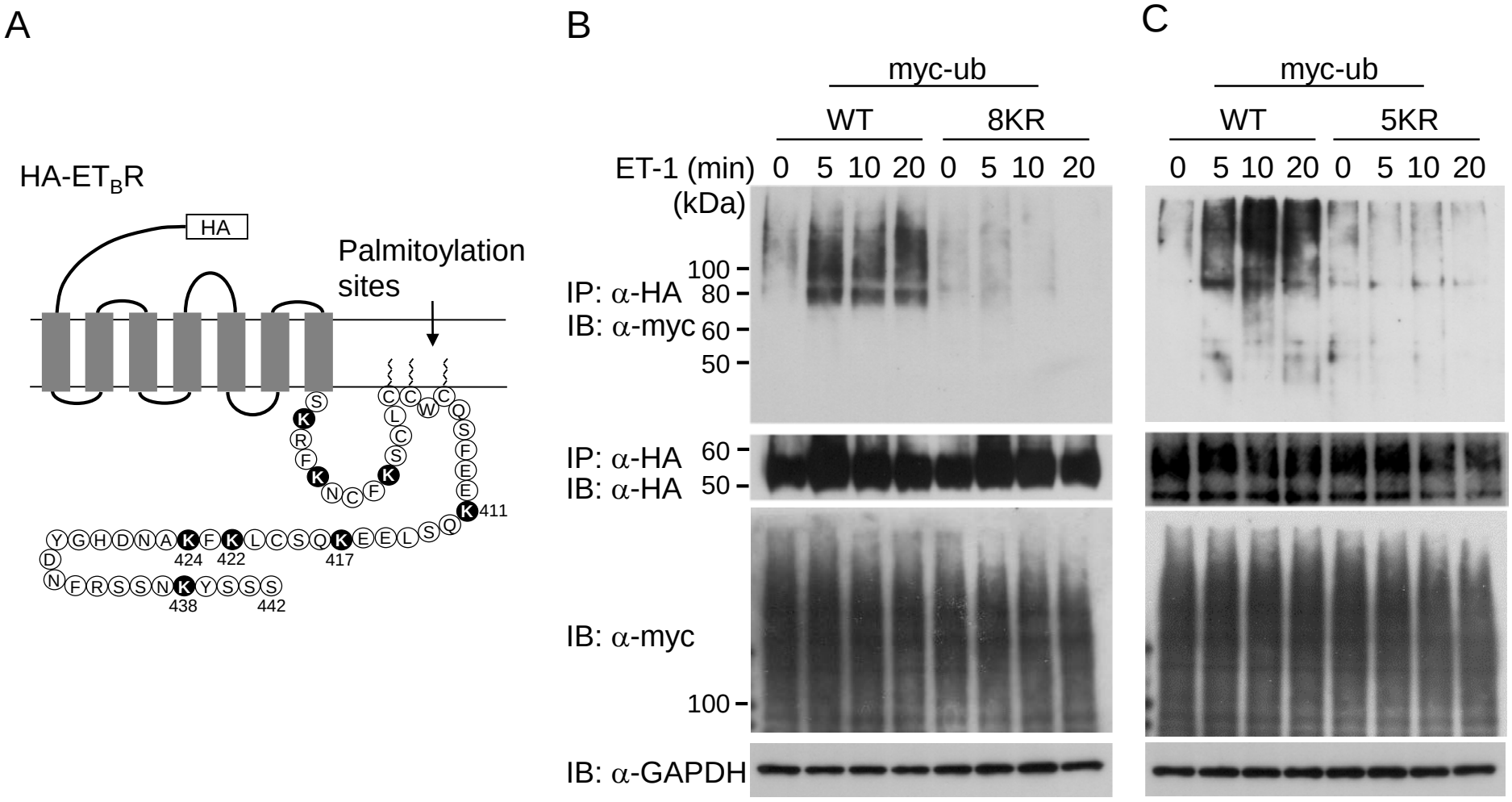
A
HA-ET$_B$R
HA
Palmitoylation sites
424
422
417
438
442
411
B
myc-ub
WT
8KR
ET-1 (min) 0 5 10 20 0 5 10 20
(kDa)
100
80
60
50
IP: α-HA
IB: α-myc
IP: α-HA
IB: α-HA
IB: α-myc
IB: α-GAPDH
C
myc-ub
WT
5KR
0 5 10 20 0 5 10 20

Figure 4

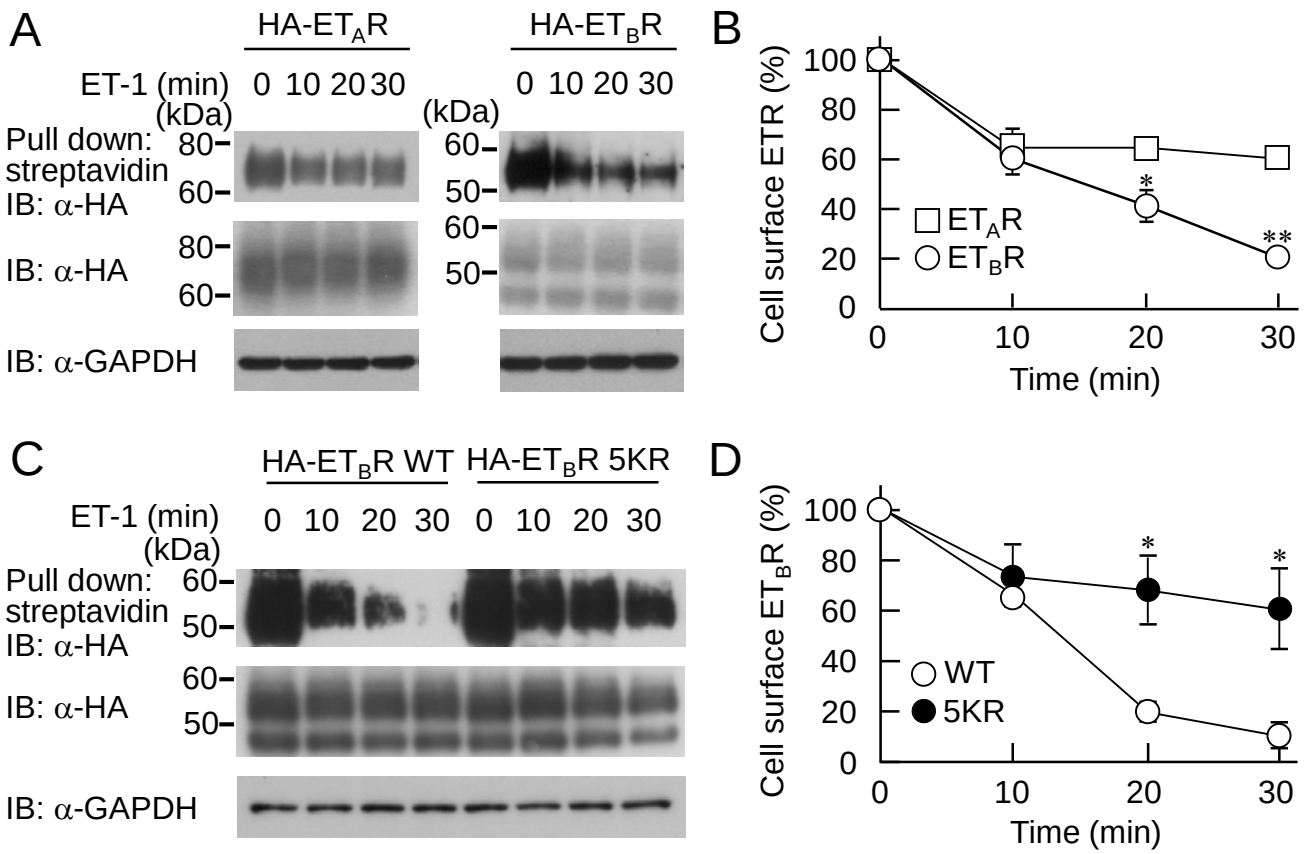
A
HA-ETAR
HA-ETBR
ET-1 (min)
0 10 20 30
0 10 20 30
(kDa)
(kDa)
Pull down: streptavidin
IB: α-HA
IB: α-HA
IB: α-GAPDH
80
60
60
50
80
60
60
50
B
Cell surface ETR (%)
100
80
60
40
20
0
ETAR
ETBR
*
**
0
10
20
30
Time (min)
C
HA-ETBR WT
HA-ETBR 5KR
ET-1 (min)
0 10 20 30 0 10 20 30
(kDa)
Pull down: streptavidin
IB: α-HA
IB: α-HA
IB: α-GAPDH
60
50
60
50
D
Cell surface ETBR (%)
100
80
60
40
20
0
WT
5KR
*
*
0
10
20
30
Time (min)

Figure 5

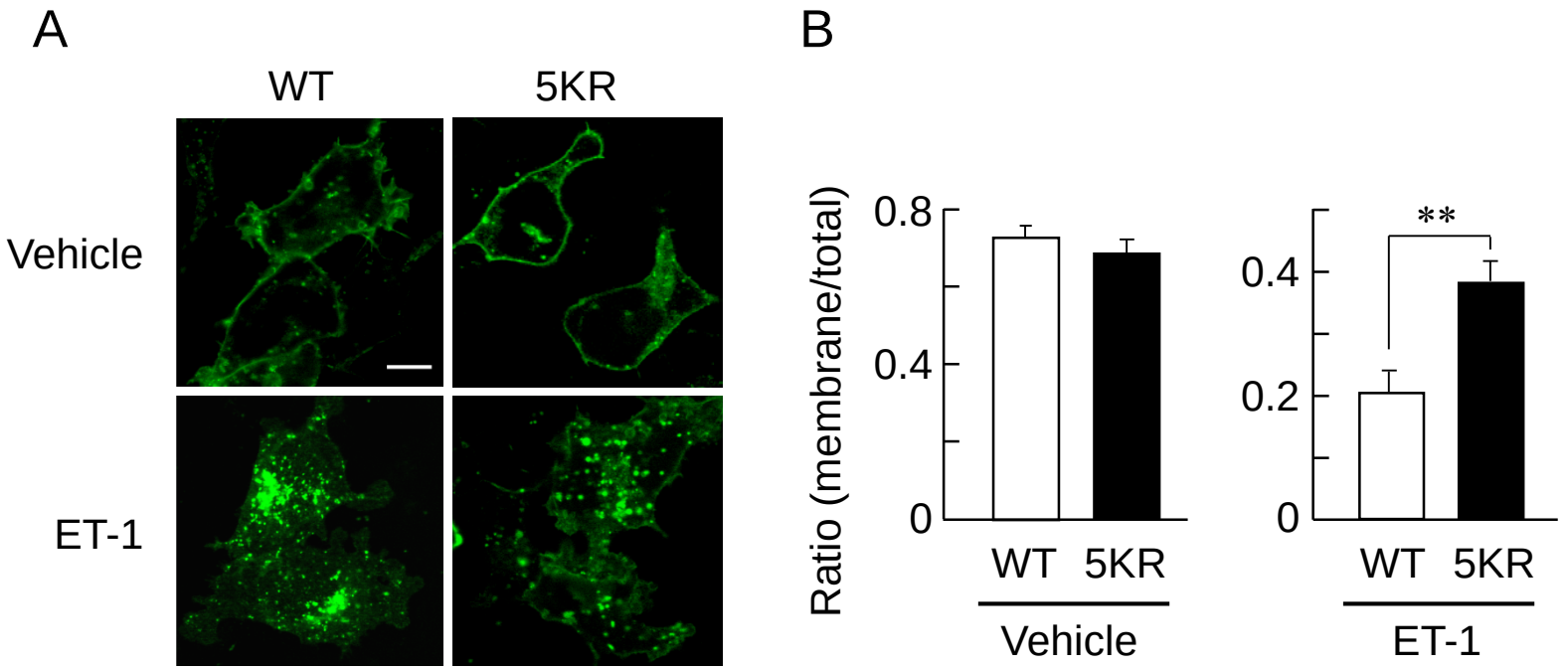
A
WT
5KR
Vehicle
ET-1
B
Ratio (membrane/total)
0.8
0.4
0
WT
5KR
Vehicle
**
0.4
0.2
0
WT
5KR
ET-1

Figure 6

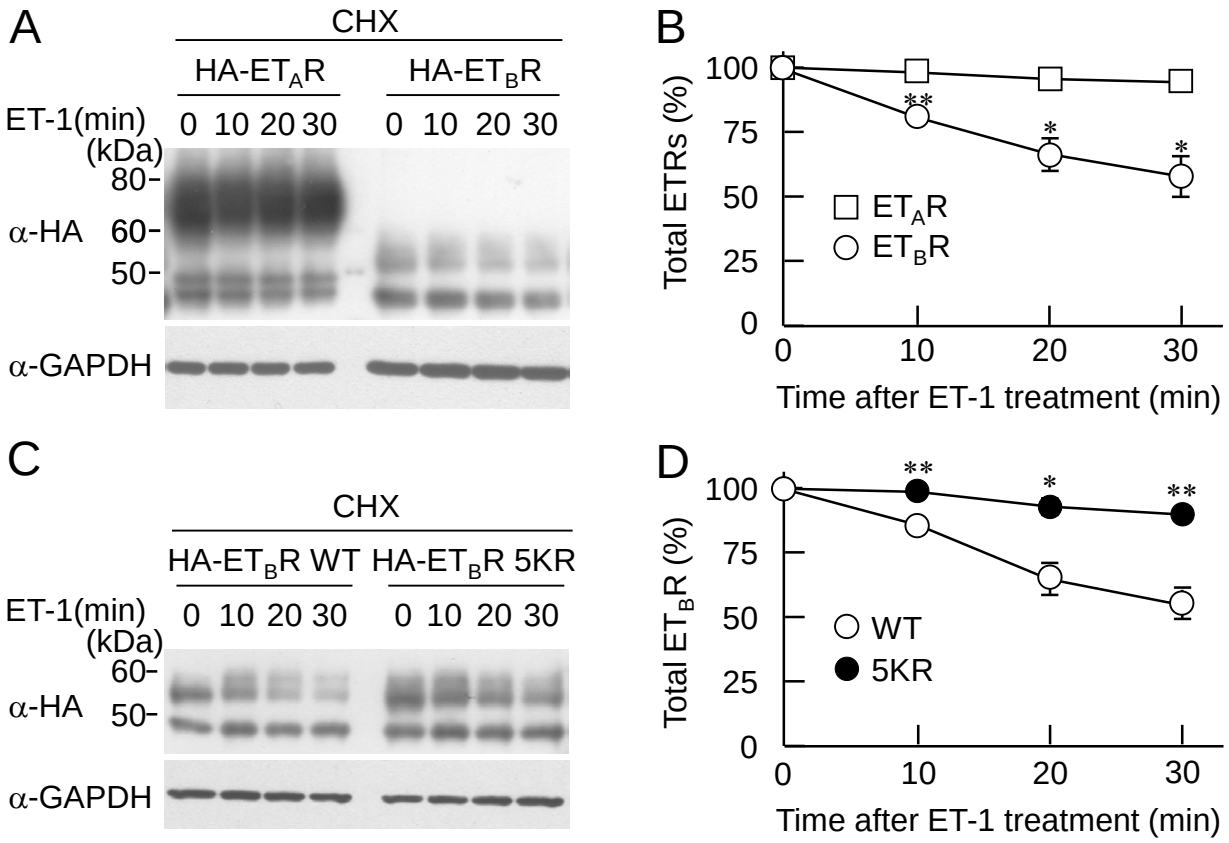
A
CHX
HA-ETAR
HA-ETBR
ET-1(min)
0 10 20 30
0 10 20 30
(kDa)
80
60
50
α-HA
α-GAPDH
B
Total ETRs (%)
100
75
50
25
0
**
*
*
ETAR
ETBR
0
10
20
30
Time after ET-1 treatment (min)
C
CHX
HA-ETBR WT
HA-ETBR 5KR
ET-1(min)
0 10 20 30
0 10 20 30
(kDa)
60
50
α-HA
α-GAPDH
D
Total ETBR (%)
100
75
50
25
0
**
*
**
WT
5KR
0
10
20
30
Time after ET-1 treatment (min)

Figure 7

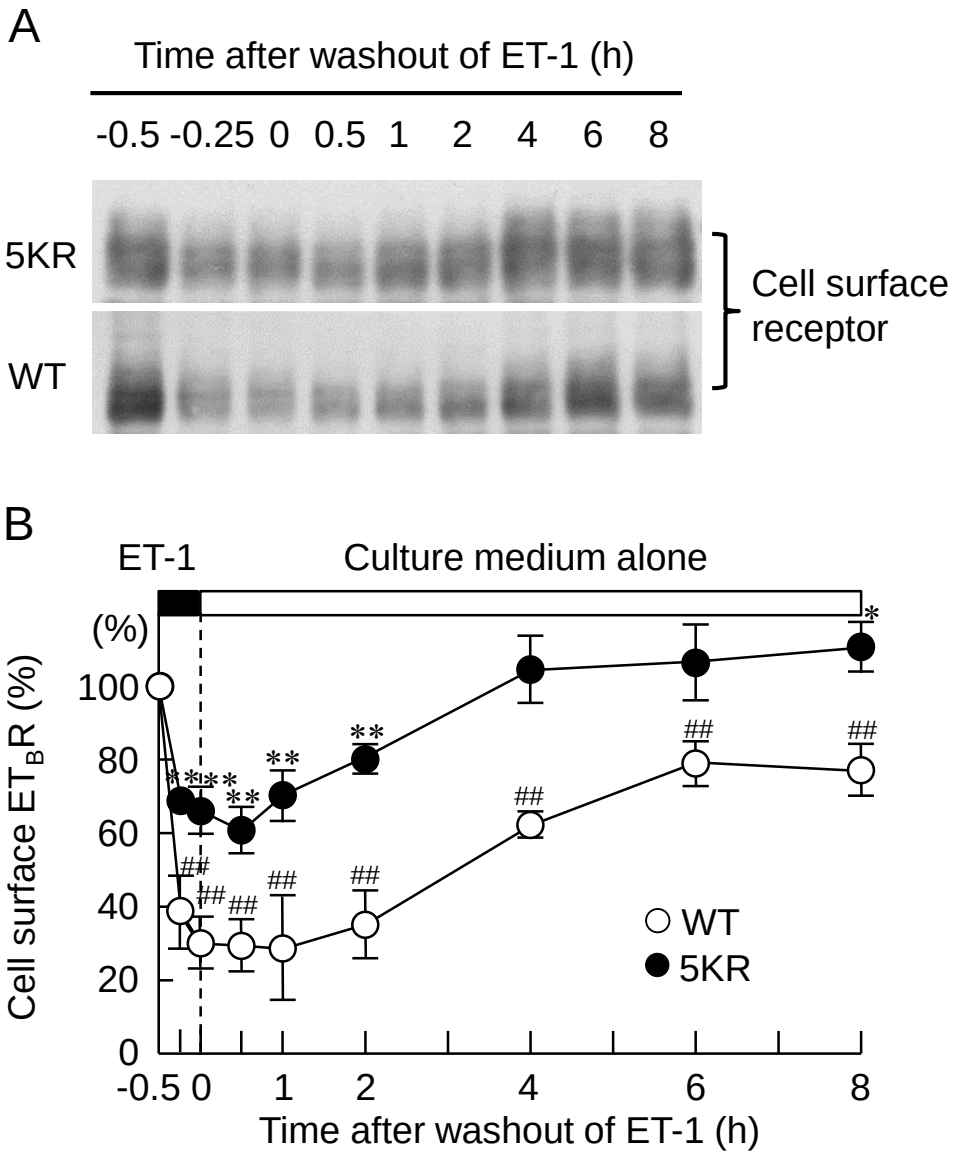
A
Time after washout of ET-1 (h)
-0.5 -0.25 0 0.5 1 2 4 6 8
5KR
WT
Cell surface receptor
B
ET-1
Culture medium alone
(%)
Cell surface ETBR (%)
100
80
60
40
20
0
-0.5 0 1 2 4 6 8
Time after washout of ET-1 (h)
WT
5KR

Figure 8

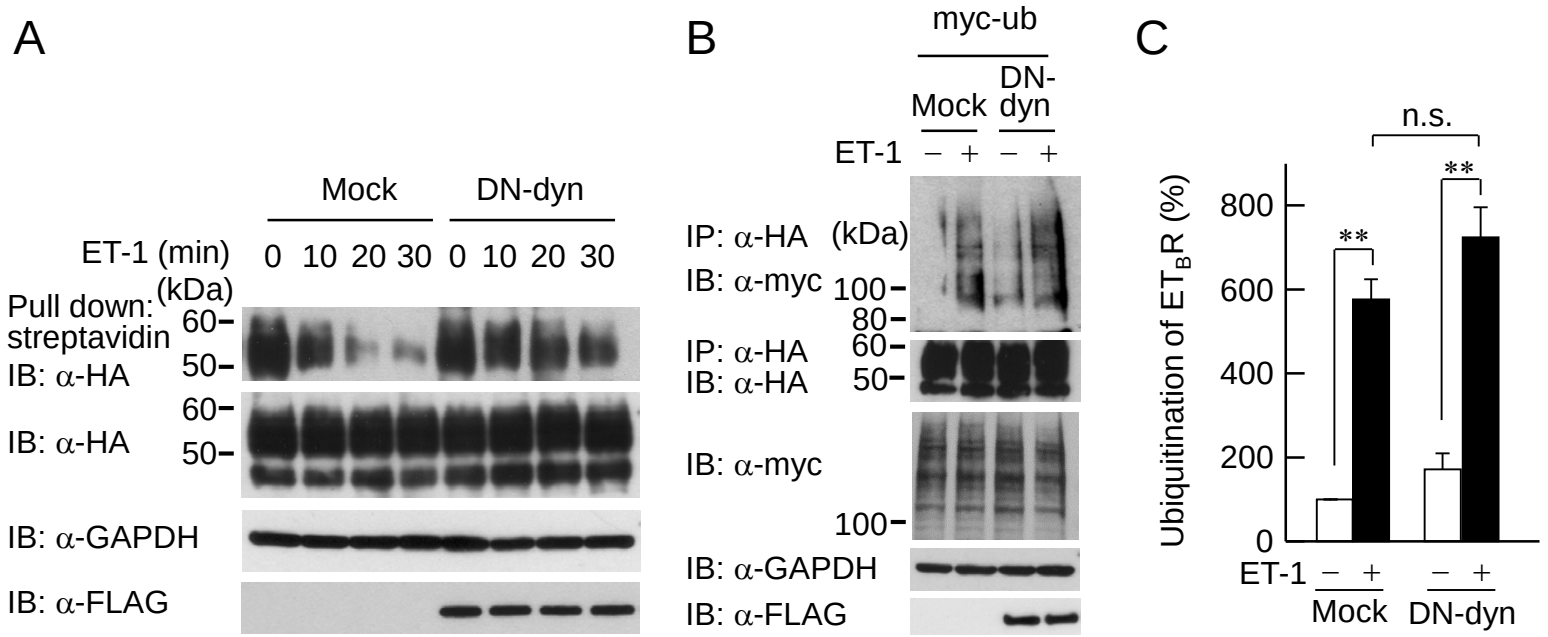
A
Mock
DN-dyn
ET-1 (min)
0 10 20 30 0 10 20 30
(kDa)
Pull down: streptavidin
IB: α-HA
60
50
IB: α-HA
60
50
IB: α-GAPDH
IB: α-FLAG
B
myc-ub
Mock
DN-dyn
ET-1 − + − +
IP: α-HA
(kDa)
IB: α-myc
100
80
IP: α-HA
60
IB: α-HA
50
IB: α-myc
100
IB: α-GAPDH
IB: α-FLAG
C
n.s.
**
**
Ubiquitination of ET$_B$R (%)
800
600
400
200
0
ET-1 − + − +
Mock
DN-dyn

Figure 9

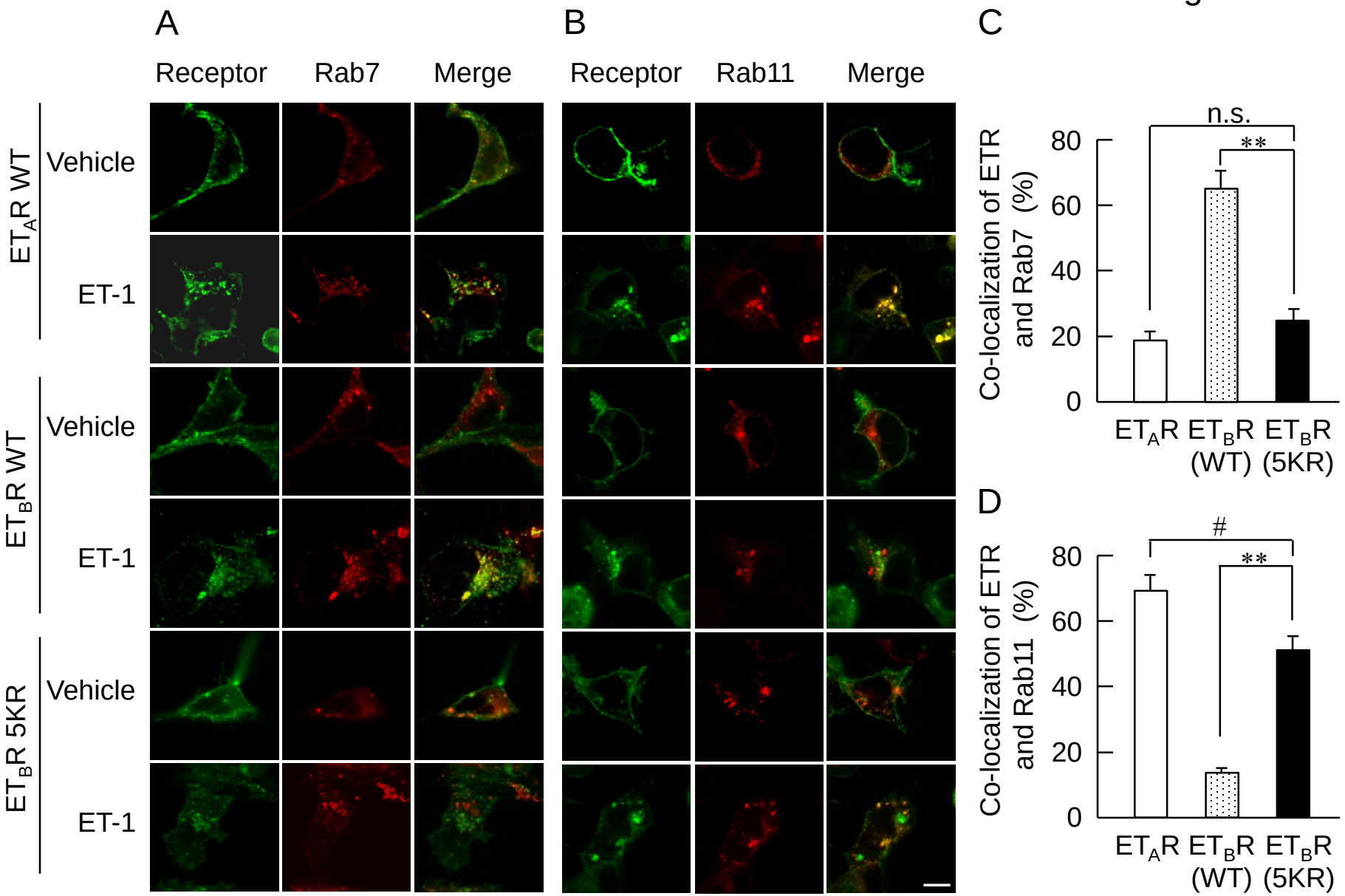
A
Receptor
Rab7
Merge
B
Receptor
Rab11
Merge
ETAR WT
Vehicle
ET-1
ETBR WT
Vehicle
ET-1
ETBR 5KR
Vehicle
ET-1
C
n.s.
**
Co-localization of ETR and Rab7 (%)
0
20
40
60
80
ETAR
ETBR (WT)
ETBR (5KR)
D
#
**
Co-localization of ETR and Rab11 (%)
0
20
40
60
80
ETAR
ETBR (WT)
ETBR (5KR)

Figure 10

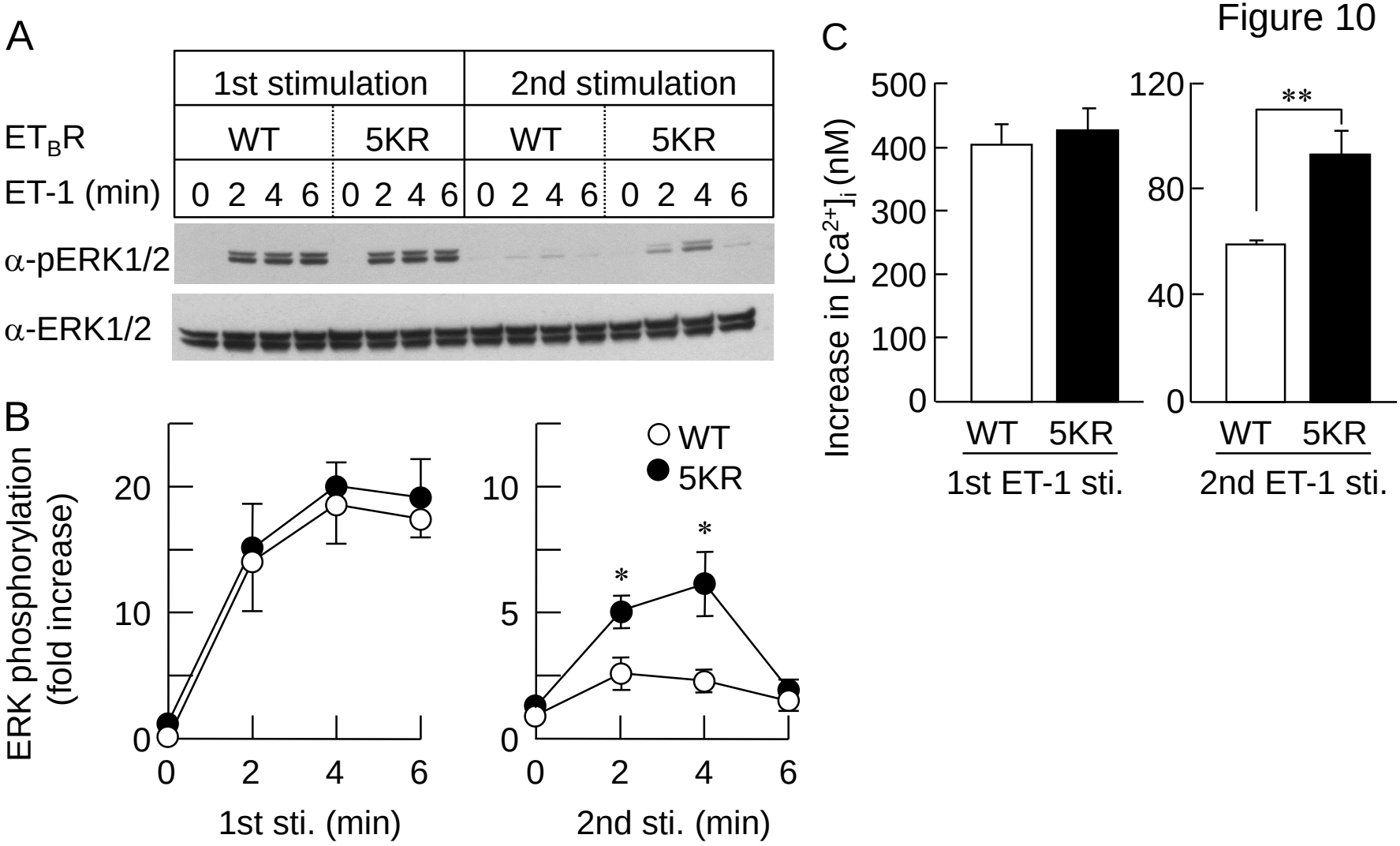
A
1st stimulation
2nd stimulation
ET$_B$R
WT
5KR
WT
5KR
ET-1 (min)
0 2 4 6 0 2 4 6 0 2 4 6 0 2 4 6
α-pERK1/2
α-ERK1/2
B
ERK phosphorylation (fold increase)
20
10
0
0 2 4 6
1st sti. (min)
WT
5KR
10
5
0
*
*
0 2 4 6
2nd sti. (min)
C
Increase in [Ca^{2+}]$_i$ (nM)
500
400
300
200
100
0
WT 5KR
1st ET-1 sti.
120
80
40
0
**
WT 5KR
2nd ET-1 sti.

Figure 11

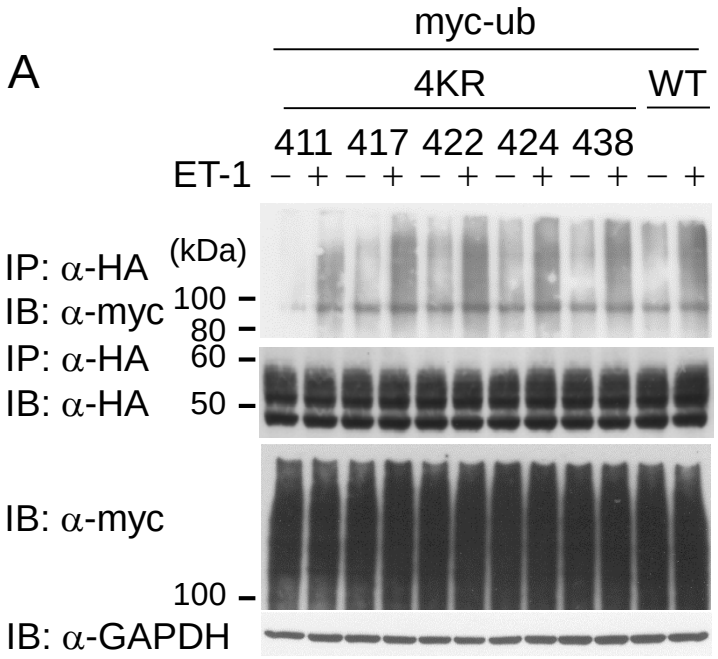
A
myc-ub
4KR
WT
411 417 422 424 438
ET-1 − + − + − + − + − + − +
(kDa)
IP: α-HA
IB: α-myc
IP: α-HA
IB: α-HA
IB: α-myc
IB: α-GAPDH
100
80
60
50
100

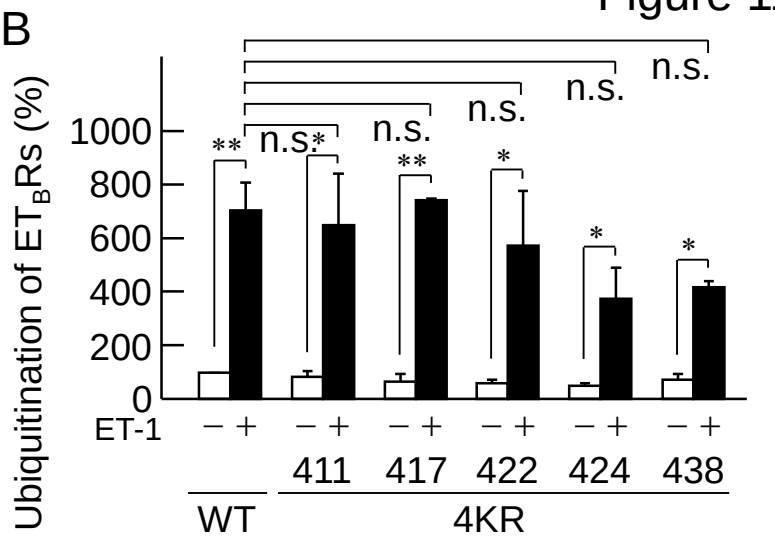
B
Ubiquitination of ETBRs (%)
1000
800
600
400
200
0
n.s.
n.s.
n.s.
n.s.
n.s.
**
*
**
*
*
*
ET-1 − + − + − + − + − + − +
411 417 422 424 438
WT
4KR

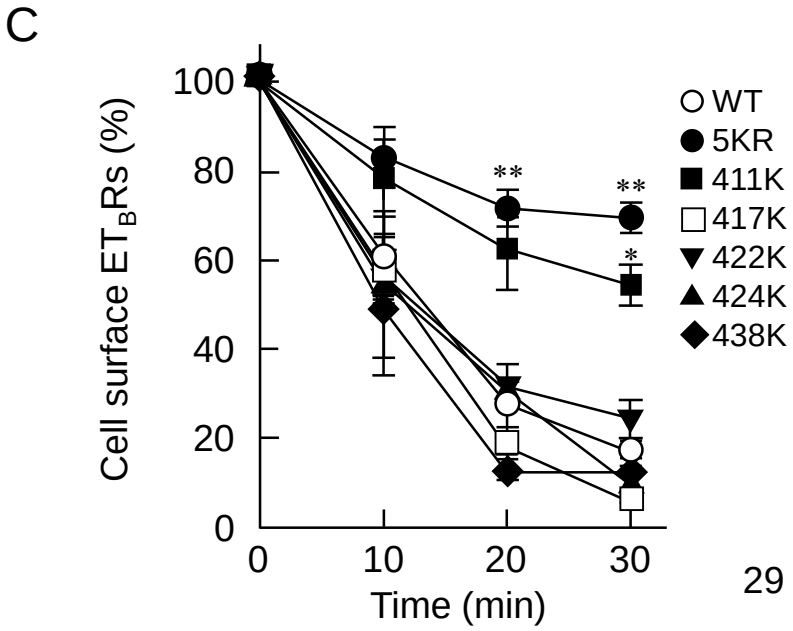
C
Cell surface ETBRs (%)
100
80
60
40
20
0
0
10
20
30
Time (min)
WT
5KR
411K
417K
422K
424K
438K
**
**
*

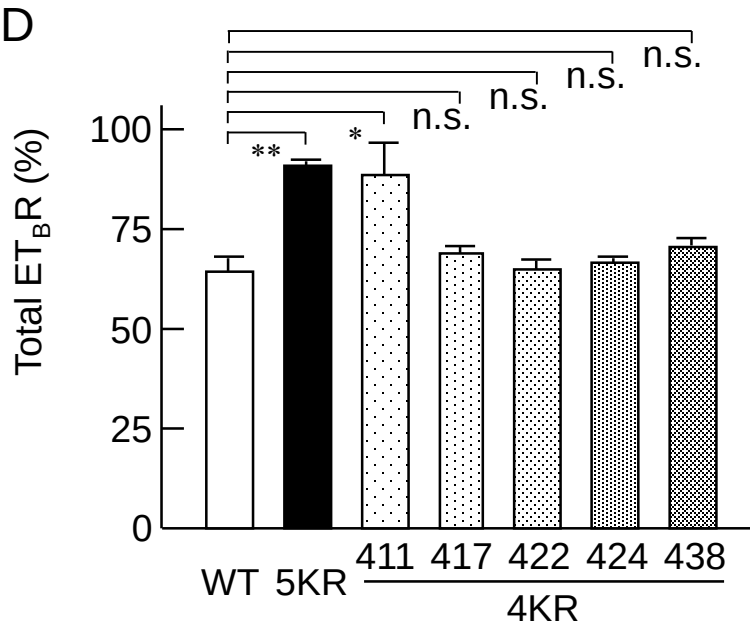
D
Total ETBR (%)
100
75
50
25
0
n.s.
n.s.
n.s.
n.s.
**
*
WT 5KR 411 417 422 424 438
4KR

Figure 12

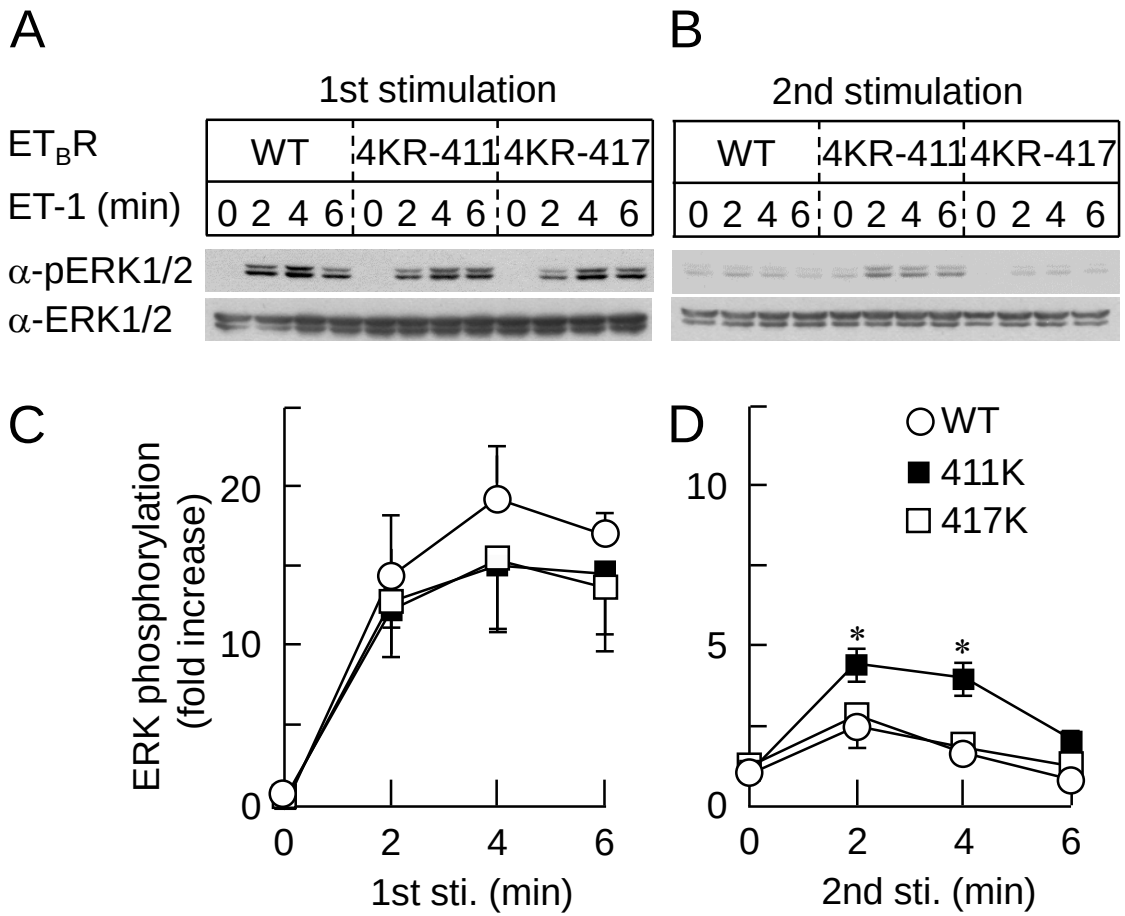
A
B
1st stimulation
2nd stimulation
ET$_B$R
WT
4KR-411
4KR-417
ET-1 (min)
0 2 4 6 0 2 4 6 0 2 4 6
α-pERK1/2
α-ERK1/2
C
ERK phosphorylation (fold increase)
20
10
0
0 2 4 6
1st sti. (min)
D
WT
411K
417K
10
5
0
*
*
0 2 4 6
2nd sti. (min)